IEEE Access
Multidisciplinary ⋮ Rapid Review ⋮ Open Access Journal

Received 19 July 2023, accepted 4 August 2023, date of publication 18 August 2023, date of current version 23 August 2023.

Digital Object Identifier 10.1109/ACCESS.2023.3304419

SURVEY

CubeSat Communication Subsystems: A Review of On-Board Transceiver Architectures, Protocols, and Performance

AMR ZEEDAN AND TAMER KHATTAB, (Senior Member, IEEE)
Department of Electrical Engineering, Qatar University, Doha, Qatar

Corresponding author: Amr Zeedan (amr.zeedan@qu.edu.qa)

The work of Amr Zeedan was supported by the Qatar National Research Fund (QNRF) (a member of Qatar Foundation, QF), under Award GSRA8-L-2-0523-21052. The work of Tamer Khattab was supported by the QNRF (a member of QF) under Award AICC03-0530-200033.

ABSTRACT Small satellite communications recently entered a period of massive interest driven by the uprising commercial and civil space applications and motivated by various technological advances. Miniaturized satellites, known as CubeSats, are particularly attractive due to their low development and deployment costs which makes them very promising in playing a central role in the global wireless communication sector with numerous applications ranging from Earth imaging and space exploration to military applications. Moreover, constellations of CubeSats in low Earth orbits (LEOs) can meet the increasing demands of global-coverage low-cost high-speed flexible connectivity. However, this requires innovative solutions to overcome the significant challenges facing high-data-rate low-power space communications. This paper provides a comprehensive review of the design, protocols, and architectures of state-of-the-art CubeSat communication subsystems with a particular focus on their baseband structures. The literature is surveyed in detail to identify all design, testing, and demonstration stages as well as accurately describe the systems' architectures and communication protocols. The reliability, performance, data rate, and power consumption of the reviewed systems are critically compared and evaluated to understand the limitations of existing CubeSat transceivers and identify directions of future developments. It is concluded that CubeSat communication subsystems still face many challenges, namely the development of energy-efficient high-speed transceivers that satisfy CubeSats' cost, mass, size, and power constraints. Nevertheless, several directions for improvements are proposed such as the use of improved channel coding algorithms, Field Programmable Gate Arrays (FPGAs), beamforming, advanced antennas, deployable solar panels, and transition to higher frequency bands. By providing a concrete summary of existing CubeSat on-board transceiver designs and critically evaluating their unique features and limitations as well as offering insights about potential improvements, the review should aid CubeSat developers, researchers, and companies to develop more efficient high data rate CubeSat transceivers.

INDEX TERMS Baseband architectures, RF transceivers, communication protocols, low-power communications, SDR, FPGA, CubeSat, nanosatellites, low Earth orbit (LEO) satellites.

I. INTRODUCTION

Satellite communications play a critical role in the global telecommunication systems especially with the development of smart homes, smart cities, electric vehicles, and the increasing use of internet of things (IoT) platforms [1]. There are approximately 2000 satellites, excluding CubeSats, orbiting the Earth serving many locations worldwide [1], [2]. Conventionally, satellites are large and have geosynchronous orbits [3]. However, recently, many companies are moving towards building constellations of smaller and cheaper satellites (e.g., CubeSats) in low Earth orbits (LEOs) that can provide communication services to both urban and rural areas and meet the increasing demand of low cost high

The associate editor coordinating the review of this manuscript and approving it for publication was Zihuai Lin.

data rate connectivity [3]. Compared to geosynchronous satellites, CubeSats have much lower development costs, shorter development cycles, more flexible services, and lower communication latency [4]. Moreover, CubeSats have many applications such as remote sensing, Earth imaging, communication services, military and civil applications, and space exploration [5], [6]. Therefore, the development of small-size high-data rate energy-efficient transceivers for CubeSats is becoming ever more critical to meet the requirements of such emerging applications. However, providing high speed communications using CubeSats requires pioneering solutions to overcome many hurdles; power consumption, data rate, and form factor (size and weight) constraints.

A. POSITIONING WITHIN EXISTING SURVEYS

Although there are several review papers on CubeSats and satellites' communication systems [7], [8], [9], [10], [11], [12], there are little or no comprehensive reviews on the baseband design specifications, protocols, and architectures of CubeSats' transceivers. Consequently, this paper fills in this gap in the literature by reviewing and evaluating state-of-the-art CubeSat on-board transceivers, with a particular focus on their baseband architectures, and their resulting performance in terms of power consumption, data rate, and bit error rate. The paper provides a well-grounded starting point for researchers and developers working on custom designs for CubeSat transceivers. The review develops a firm understanding of state-of-the-art technologies in the field and paves the path for introducing improvements and upgrades on existing systems.

A significant challenge in conducting this review is the fact that most papers in the literature focus on the RF-end (radio frequency), link budget, and bandwidth requirements rather than on the design details of the baseband system and its optimization and power requirements. Consequently, thorough investigation of the literature is required to extract the baseband architecture designs and protocols and evaluate them. Table 1 provides a comparison between this review paper and several previous reviews on CubeSats, illustrating the uniqueness of this review. Mainly, the present review is different from existing reviews in the regard that it reviews the baseband designs, architectures, and technologies of CubeSat transceivers, investigates the power consumption, data rate, performance, and limitations of current systems, and proposes directions for future developments.

TABLE 1. Comparison between the scope of existing reviews with this review.

Reference	Year	Scope
[7]	2017	Antenna designs and developments for CubeSats.
[8]	2018	Developments in advanced antennas for small satellites.
[9]	2018	CubeSat mission goals, constellation topologies, and communication protocols.
[10]	2019	Operational features of small satellites, CubeSat services and applications, and network protocols.
[11]	2020	CubeSat constellations and coverage, channel modelling, link budget, and upper layer issues.
[12]	2021	Advances in satellite (mainly large satellites) communications, applications, medium access, and prototyping.
This Paper	**2023**	**Baseband designs, architectures, and technologies of CubeSat transceivers. Performance, power consumption, and data rate investigation. Limitations of current systems and directions for developments.**

B. CONTRIBUTIONS OF THIS PAPER

The contribution of this review is three-fold. First, the paper provides a comprehensive and detailed review of recent CubeSat communication subsystem designs focusing on the baseband architectures and corresponding algorithms that optimize the performance of the baseband and RF modem. The reviewed CubeSat transceivers are categorized into four categories based on the adopted design approach. Second, the paper provides critical evaluation of the reviewed systems to accurately compare their performance and understand their limitations and shortcomings. Third, the paper provides insights into future trends, technologies, and directions for CubeSat communications development both from a research and commercial perspectives. The contributions of this paper can hence be summarized as follows:

1) A comprehensive review of state-of-the-art CubeSat on-board transceiver designs, architectures, and protocols (Section III).
2) Categorization of the systems into four categorizes based on the design approach (Section III).
3) Critical analysis and evaluation of the reviewed systems (Section IV).
4) Analysis of the general features of each design approach (Section V).
5) Insights about the status of CubeSat communication subsystems in terms of employed technologies, performance, and limitations (Section V).
6) Proposal of several directions for future developments (Section V).

C. SURVEY ORGANIZATION

This paper is organized as follows: a compact background is given in Section II providing the necessary knowledge about nanosatellites, their development, applications, and the main challenges facing CubeSat communications. Section III constitutes the primary literature review of the baseband designs and architectures employed in CubeSat transceivers. In the fourth Section, the performance of the reviewed systems is evaluated and compared in terms of power

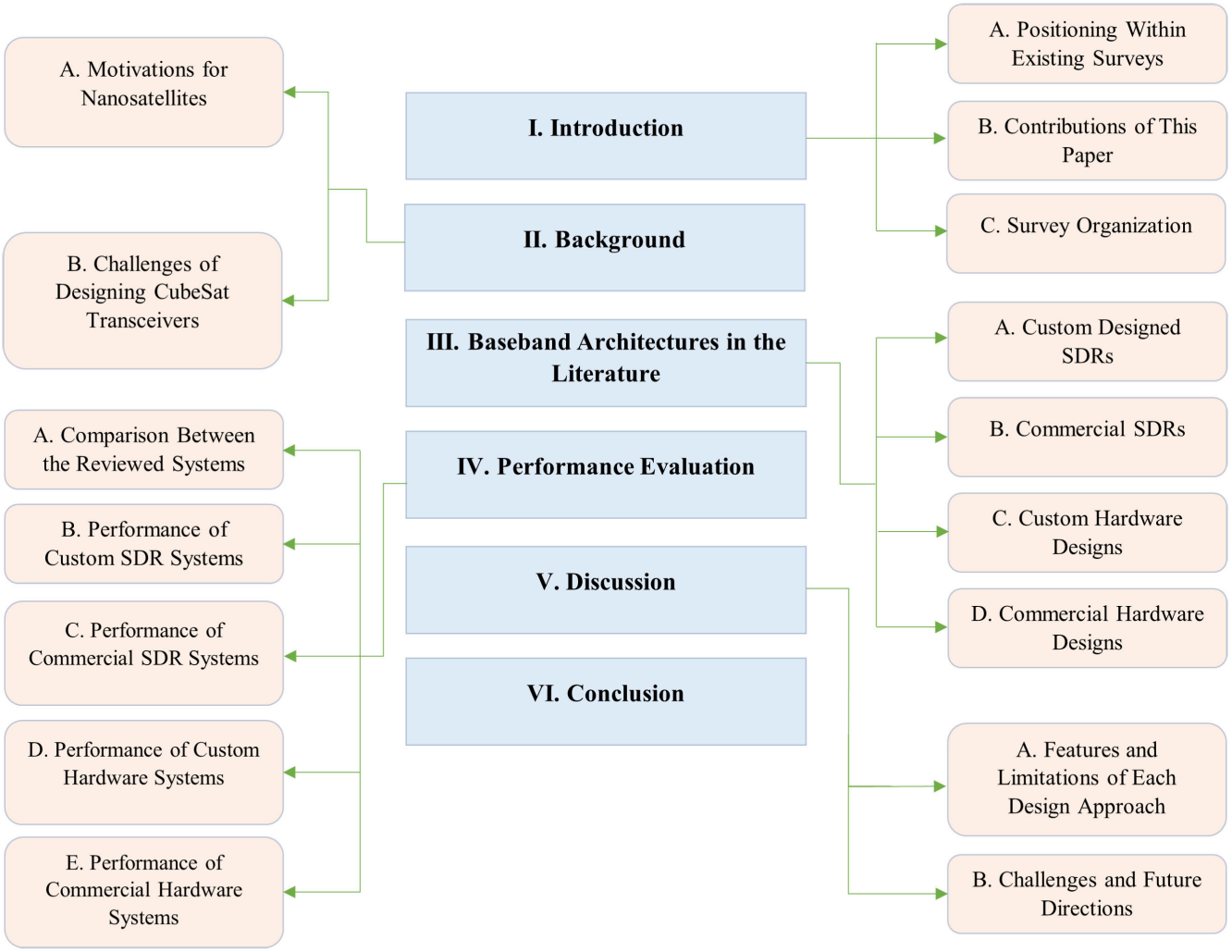

FIGURE 1. Structure of the paper.

consumption, data rate, frequency bands, and other metrics. Section V is a critical discussion of existing CubeSat transceivers, their limitations, and potential directions for future developments. The last Section summarizes the review and concludes the paper. Fig. 1 illustrates the structure and organization of this review.

II. BACKGROUND

A. MOTIVATIONS FOR NANOSATELLITES

Nanosatellites are used for various applications from Earth imaging to interplanetary space exploration [10]. Starting from 2014, a large percentage of nanosatellites are being launched for commercial purposes [13]. Therefore, nanosatellites are no longer exclusively being used for research and technology demonstration but also for providing telecommunication services, competing with traditional satellites [14], [21]. Consequently, the development of reliable small-size high-speed energy-efficient transceivers for nanosatellites is becoming ever more critical to serve the anticipated telecommunication needs. Due to the very small size, mass, and consequently limited energy resources available on CubeSats, the transceivers developed must be highly efficient [15].

One of the main motivations for the increased interest in CubeSats is their low cost compared to large satellites. A conventional satellite costs between 150 to 350 million dollars [9]. A CubeSat on the other hand costs less than 200,000 dollars [9]. This makes CubeSats accessible to companies of various sizes, which is reflected in the considerable increase in the number of civil and commercial CubeSat operators in recent years. This is aside from the much shorter development cycles needed for developing and launching a CubeSat which could be under a year, while a large satellite requires between 5 to 15 years [9]. However, this comes at the expense of shorter lifetimes for CubeSats in space which are between 2 to 4 years of operation, but at the same time this gives the opportunity for incorporating up to date technologies in the CubeSat that replaces the old one in the constellation [6]. Thus,

the telecommunication services offered by CubeSats can be significantly improved by constantly making use of latest technologies. CubeSats also feature several other advantages over conventional satellites such as risk distribution, flexible services, smaller sizes, lower communication latency, lower energy consumption, and lower human power needed [6], [9].

B. CHALLENGES OF DESIGNING CubeSat TRANSCEIVERS

Firstly, the very small size and mass of the CubeSat limits the physical dimensions of the communication subsystem [16]. That is, every part of the system must be designed to be as compact and as light as possible including the antenna [17]. Secondly, due to the small size of the CubeSat, the available energy resources such as batteries and solar panels are very limited, and hence, the generated power has to be distributed efficiently over the different subsystems of the CubeSat [17], [18]. At the same time, this cannot come at the expense of data rate or link quality, especially if the CubeSat is intended for providing communication services. In such case, the quality and data rate are essential to the success of the service provider. Another constraint is the low-cost requirement of the CubeSat [19]. Since a major feature of CubeSats is their low development costs, the components and materials used cannot be very expensive. Moreover, the materials used must be able to withstand the various thermal and radiation effects of the orbital environment [8].

As CubeSats evolved from being used for research purposes to commercial and civil applications, their communication subsystems witnessed rapid developments in almost all aspects [20], [22], [23]. Higher frequency bands such as the S-band (2-4 GHz) and X-band (8-12 GHz) became more widely used due to the developments in the commercially available monolithic microwave integrated circuits [10]. With the use of such high frequency bands, data rates were able to reach 100 kbps to 1 Mbps [10]. Higher data rates require utilization of higher frequency bands like Ku (12-18 GHz), K (18-27 GHz), and Ka-band (27-40 GHz) [9]. These bands are still emerging technologies for small satellites due to the required antennas and power requirements [20]. Another major aspect of development is the increasing move towards digital implementation of the communication subsystem or Software Defined Radios (SDRs). This transition is driven by the need for reconfigurable and flexible radio communications and by the advances in the corresponding enabling technologies such as Digital Signal Processors (DSPs) and Field Programmable Gate Arrays (FPGAs) [10]. The challenge of this digital approach is the power consumption [24]. That is why FPGAs are preferred for implementation, especially for higher data rates in the Ka-band since they can perform computationally intensive tasks in parallel and with better efficiency every clock cycle [25], [26]. Moreover, FPGAs allow prototype testing and optimization of the proposed circuit architecture before a hardware-fixed application-specific integrated circuit (ASIC) is manufactured [27]. This approach greatly saves time and money as it allows testing many versions of the project before the final ASIC manufacturing process. FPGAs also offer reconfigurability while employing the system. For example, transitions between different modulation or coding schemes can be easily realized when the system is implemented on an FPGA. Therefore, the communication system can be made more efficient by switching to different architectures based on the requirements and by employing the same hardware resources. Moreover, the response time can be controlled on an FPGA if compared to a standard central processing unit (CPU) [24]. The required algorithm that ensures a fixed and short response time can be implemented on the FPGA and then be employed after testing [28]. An IC designed this way will have a short response time and efficient power consumption.

FPGAs' configurability and speed have made them a common platform for realizing SDRs [29]. However, the SDR flexibility comes at the cost of increased software complexity due to the various algorithms that need to be implemented for code generation, debugging, etc. [30]. SDRs are also generally more expensive than single-chip highly integrated transceivers [31]. Therefore, SDRs are not necessarily the best option for wireless systems, a completely hardware radio or a mixed hardware-software co-design may offer a more efficient option depending on the application [32], [33].

III. BASEBAND ARCHITECTURES IN THE LITERATURE

There are various approaches for designing a CubeSat communication subsystem. One of the most common and trending approaches is to utilize the concept of SDR to custom-design a reconfigurable transceiver that meets the specific requirements of the CubeSat mission [32]. Such designs are categorized as custom designed SDRs. In this approach, the developer typically customizes the architecture of the system and the algorithms used for the different functions. Another design approach is to base the communication system on some already existing SDR platform that is commercially available. Therefore, the required components and resources are already existing, and the design is more concerned with utilizing the available resources to optimally implement the desired application. This is categorized as commercial SDR. The more conventional design approach is to use hardware components to implement the transceiver. As is the case with SDR, there are also custom hardware designs and commercial hardware designs, where in the later the hardware components used are commercial off-the-shelf (COTS) components rather than custom designed hardware components. The review is thus divided into four Subsections based on the design approach category. In each Subsection, the relevant works falling under that category are reviewed in terms of the transceiver design and implementation with a particular focus on the baseband architecture. Before proceeding with the baseband architectures review, it is critical to briefly discuss some commonly used communication protocols in CubeSat missions.

DVB-S2 Standard: DVB-S2 is an abbreviation for Digital Video Broadcasting – Satellite – second generation [34]. It is a standard for satellite communications that defines a modulation and channel coding system suitable for a variety of satellite applications [34]. DVB-S2 supports a variety of modulation schemes. It employs LDPC coding concatenated with an outer BCH (Bose-Chaudhuri-Hocquenghem) code, with various possible rates, for its channel coding [35]. Also, DVB-S2 includes a frame header that can be used for estimating the carrier offset due to Doppler shift [35]. The DVB-S2 link-layer protocol supports 28 different modulation and coding schemes [34]. The 28 different options are based on the valid combinations between one of the four modulation schemes, which are QPSK, 8-PSK, 16-APSK, and 32-APSK, and one of the 12 possible coding rates (1/4 - 9/10) of LDPC concatenated with BCH [35]. DVB-S2 supports adaptive coding and modulation, which allows the system to adapt the transmission parameters based on the channel conditions, improving link reliability and efficiency. It also supports multiple input streams, enabling the simultaneous transmission of multiple services or data streams over a single satellite carrier [35]. DVB-S2 has gained widespread adoption in various applications including satellite broadcasting, broadband satellite internet, and CubeSats [36]. Its improved efficiency and performance make it a preferred choice for delivering high-quality video, audio, and data services over satellite links [36].

CCSDS Protocols: Even though there are specifically tuned standards for satellites such as those of the CCSDS (Consultive Committee for Space Data systems), those standards are not as practical as DVB-S2 due to the lack of commercial modems that can realize them [37]. In fact, the CCSDS protocol suite covers a wide range of functions including data packaging, file transfer, telemetry, commanding, and network communication [38]. The CCSDS File Delivery Protocol (CFDP) defines a standardized format for reliable and efficient file transfer in space systems. CFDP allows for the segmentation of large files into smaller units called File Data Units (FDUs), which are transmitted, acknowledged, and reassembled at the receiving end [39]. CFDP includes mechanisms for error detection, retransmission, and flow control to ensure reliable delivery of files. The CCSDS Space Packet Protocol (SCSP) is used for encapsulation, fragmentation, and transmission of data in space systems [39]. It defines a packet-based structure called Space Packets, which encapsulate the data and associated metadata. SCSP provides mechanisms for error control, congestion control, and synchronization [38]. It is widely used for data exchange and communication between spacecraft subsystems and ground stations [40]. Finally, the CCSDS Telemetry Channel Access Protocol (TCAP) is designed for efficient access to telemetry data from space systems. TCAP provides a standardized method for requesting and receiving telemetry data from a spacecraft [41]. It defines procedures for data query, subscription, and transfer, enabling efficient data retrieval while managing the limited resources of the spacecraft and ground systems [41]. The CCSDS protocol suite also includes other protocols such as Command and Data Encoding (C&DH), Time Code Formats, and Space Link Services [42]. These protocols address various aspects of space communication, data encoding, time synchronization, and spacecraft commanding [43]. They have been widely adopted in numerous space missions, ensuring consistent operations across the space industry [44]. CCSDS protocols play a significant role in CubeSat missions by providing standardized and interoperable communications. By adhering to these protocols, CubeSats can achieve interoperability, efficiency, and reliability, ensuring compatibility and seamless integration with other space systems [42].

For CubeSats, efficient communication protocols are crucial due to the limited CubeSat resources [41]. The CCSDS protocols, while advantageous for CubeSat communications, have certain limitations [42]. Firstly, their complexity can pose challenges for implementation and operation within the resource-constrained environment of CubeSats. The extensive protocol stack and associated software overhead may strain the limited computational capabilities and memory of CubeSat platforms [45]. Secondly, CCSDS protocols introduce additional overhead due to their comprehensive nature. This overhead includes encapsulation, error checking, synchronization, and other protocol-specific features [45]. In CubeSats, where resources such as power are limited, this can impact the efficiency of communication systems and reduce the available capacity for scientific data or mission-specific tasks [46]. Additionally, CCSDS protocols may not be optimized specifically for the low-bandwidth requirements of CubeSats, resulting in sub-optimal resource utilization and potential limitations on data transmission [42]. Furthermore, the rigid nature of CCSDS protocols may limit their flexibility and adaptability to accommodate the diverse requirements of CubeSat missions. Despite these limitations, CCSDS protocols remain widely used in CubeSat missions due to their established standards, interoperability, and compatibility with other space systems.

AX.25 Protocol: AX.25 is a communication protocol commonly used in amateur radio and satellite operations. It is an adaptation of the X.25 protocol suite for use in amateur radio applications, particularly in amateur packet radio networks utilized by CubeSats and small satellite missions [47]. AX.25 operates at the data link layer and provides a standardized framework for packet-based communication [48]. It defines the structure of data packets, including destination and source addresses, control information, and error detection bits [47]. The protocol incorporates error detection using cyclic redundancy checks to ensure packet integrity. With its simplicity and efficiency, AX.25 has become a widely adopted standard for low-bandwidth communication in amateur radio networks, making it suitable for CubeSats and similar small satellite applications [48].

TCP/IP Protocol: TCP/IP (Transmission Control Protocol/Internet Protocol) is a crucial communication protocol suite that facilitates the reliable transmission of data over interconnected networks, serving as the foundation for internet communication [49]. TCP ensures dependable, connection-oriented communication by breaking data into packets, assigning sequence numbers, and managing order and error detection [50]. IP handles packet addressing and routing, assigning unique IP addresses to devices, determining optimal paths for packet delivery, and managing packet fragmentation [50]. TCP/IP operates on a layered model, facilitating communication across different network layers and supporting various protocols for network troubleshooting and application-specific tasks [49]. This protocol suite's wide adoption, scalability, and reliability have made it instrumental in the growth and connectivity of the internet, serving as the standard for network communication worldwide. CubeSats typically rely on ground stations for data uplink and downlink, command and control, and mission operations [51]. The ground stations typically communicate with CubeSats using TCP/IP-based protocols for reliable and efficient data transfer over internet connections. TCP/IP enables the exchange of commands, telemetry, and other mission-related data between ground stations and CubeSats, facilitating mission control and data analysis [50], [51]. While CubeSats themselves do not directly implement TCP/IP on board, TCP/IP protocols play a significant role in the ground-based operations, data management, and communication infrastructure supporting CubeSat missions.

Finally, the DVB-S2, CCSDS, AX.25, and TCP/IP protocols exhibit distinct characteristics in terms of efficiency, reliability, and applicability. DVB-S2 stands out for its efficiency in data transmission. Due to its adaptive modulation and channel coding schemes, it can achieve high data rates, making it particularly well-suited for high data rate applications. However, its complexity and typically high-power consumption render it more suitable for larger satellites with abundant power resources [35]. On the reliability aspect, since CCSDS protocols are developed specifically for space communications, they prioritize robust data transfer under the challenges of the space environment [39]. With error detection, correction, and retransmission protocols, they ensure the integrity of data transmission, making them highly suitable for CubeSat missions where data accuracy is vital [38]. On the other hand, AX.25 offers a simplified yet reliable communication standard for CubeSats. Its efficiency lies in its compatibility with the constraints of amateur radio bands and its optimization for low-power communication [48]. These qualities make AX.25 well-suited for CubeSats that have particularly limited onboard power resources [48]. While TCP/IP excels in terrestrial networks, its applicability to CubeSats requires careful consideration. It offers reliable data transmission and has found use in ground stations for CubeSats [49]. However, the overhead introduced by TCP/IP's congestion control mechanisms could lead to latency concerns and potentially be less efficient for CubeSats with stringent power and bandwidth constraints [50]. Adaptation and optimization may be necessary for its onboard application. To conclude, considerations of efficiency, reliability, power constraints, and target data rate guide the selection of the most appropriate protocol for a given CubeSat mission.

A. CUSTOM DESIGNED SDRs

FPGAs are widely used in advanced state-of-the-art SDR designs for CubeSat transceivers [27]. A typical implementation of SDR is to program a DSP or an FPGA to execute all functions of filtering, error correction, framing, etc. [27]. Such functions are computationally intensive even for modern processors to efficiently utilize the available bandwidth [52]. FPGAs are able to execute such intensive tasks in parallel and more efficiently increase throughput while maintaining low power with every clock cycle [53]. Another disadvantage in using DSPs is that as the frequencies used reach S-band and above, they become inefficient in keeping up with executing the necessary functions such as filtering, encryption, and error correction [27]. In such cases, using multi-core processors becomes necessary to achieve the required throughput. However, this adds to the cost, size, power, and complexity of the system. Due to these various problems in using DSPs, Marshall Space Flight Center's SDR system, named Programmable Ultra Lightweight System Adaptable Radio (PULSAR), utilizes an FPGA in its implementation [27]. All the signal processing is performed on the FPGA using HDL. The modulation scheme used in PULSAR is QPSK (Quadrature Phase Shift Keying), operating in the S-band at a data rate of 5-10 Mbps [27]. Due to the flexibility of PULSAR design, it can operate using various types of channel coding schemes based on the requirement of the mission. These schemes are Low Density Parity Check (LDPC), convolutional (rate 1/2), and Reed-Solomon (255/223) forward error correction (FEC) codes [27]. The transmitter has digital algorithms to perform FEC and NEN (near Earth network) compatible packetization and the receiver has algorithms for performing signal recovery and error correction [27]. Although this SDR implementation provides flexibility, small size, and low power consumption, it requires very intensive computations at higher data rates and frequencies. The PULSAR SDR consumes about 1 W per each 10 Mbps of data rate [27]. Therefore, for its S-band data rate, it consumes between 0.5-1 W. Also, PULSAR has an implemented X-band transmitter, but not with an X-band receiver so not a complete system yet, that will transmit one channel of QPSK at a data rate of 110 Mbps but the S-band receiver will only be able to receive that data at 300 kbps [27]. At the current power performance of PULSAR, the X-band transmitter will consume about 11 W, which is quite high for CubeSat power standards.

Maheshwarappa et al. [54], [55] proposed an SDR architecture based on an FPGA SoC and two A9 processors paired

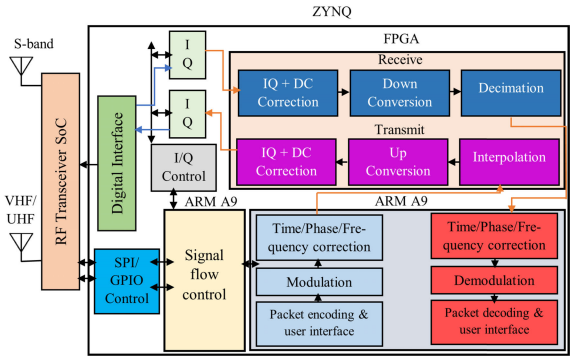

FIGURE 2. Multi-core SDR architecture used in [54].

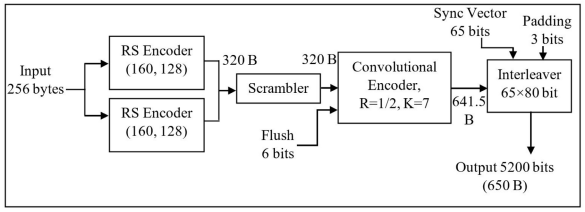

FIGURE 3. Viterbi and reed-solomon encoder [54].

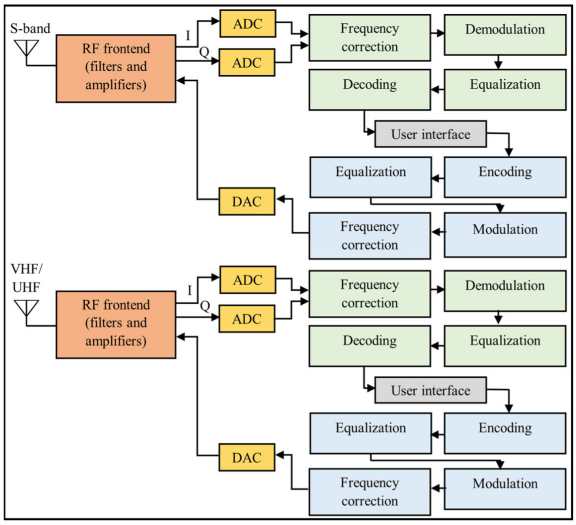

FIGURE 4. Block diagram of the triple-band transceiver [55].

with an RF programmable transceiver SoC to support multi-CubeSat communications; reception of multiple signals using a single user equipment. The proposed system is not only meant for a portable ground station but also for an on-board CubeSat transceiver. Space SDR systems offer multiple features over conventional hardware systems such as re-programmability during operation and flexibility to support multiple signals. As a result, [54] proposes a multi-core SDR architecture as shown in Fig. 2 to support multi-satellite communication. The baseband SoC contains an FPGA and two ARM dual-core Cortex A9 processors. The FPGA is responsible for the computationally intensive tasks including IQ correction, decimation, interpolation, and up/ down conversion. Modulation, packet handling, and other functions are performed on one of the A9 processors. Data and signal flow control for both the transmission and reception paths are performed on the other A9 processor. The FPGA and the processors are connected by high speed SoC Advanced eXtensible Interface (AXI) bus [54]. The modulation scheme used is BPSK. For the channel coding, an FEC scheme is adopted based on concatenated code using Viterbi (rate 1/2) and two Reed-Solomon (160, 128) blocks [54]. Fig. 3 has been developed to illustrate the operation of this FEC encoder.

Regarding the bandwidth utilization of this system, the VHF and UHF bands were used for uplink/downlink while the S-band was used for inter-satellite link [55]. VHF and UHF were used for ground communications because there were more ground facilities using them thus increasing the communication window and because it was easier and cheaper to build VHF/ UHF ground stations [55]. While the S-band was chosen for inter-satellite communication to provide higher data rate [55]. The VHF/UHF and S-band require different antennas and so separate RF front ends. The SDR analog domain consists of bandpass filters for frequency selection, frequency conversion, and variable gain control. While the SDR digital domain is responsible for the other functions from encoding, equalization, modulation, to frequency/amplitude/phase offset correction [55]. Fig. 4 has been developed to illustrate the architecture of this triple-band transceiver. The SDR system was first simulated using GNU-radio to have an understanding of the front end and back end blocks before hardware implementation. Two practical testbeds (SmartFusion2 and Zedboard) were then used to investigate the actual performance of the system under the expected space communications conditions by utilizing FUNcube-1 CubeSat and ESEO (European Student Earth Orbiter) microsatellite [55]. The initial testing on SmartFusion2 was to prove the SDR concept but it had many key SDR features missing, so the final testing was moved to Zedboard with Zipper and MyriadRF boards to overcome these problems [55]. The system was able to handle up to 19.2 kbps at a memory requirement of 1.443 GB: consuming all memory on the Zedboard (256 KB), 560 KB extendable block RAM, and 1 GB external memory [57], [58]. Higher data rates would thus require another board. The FPGA-based final implementation had a power consumption of 2.709 W [58]. This relatively high power consumption for the system's data rate is primarily due to the fact that the SDR is handling multi-satellite signals, working as a receiver for many satellites at the same time. This in part accounts for its low data rate, relatively high power consumption, and very intensive computation complexity.

Cai et al. [59] presented an FPGA-based SDR system for intersatellite communications (ISCs) suitable for small satellites using OQPSK modulation and LDPC (255, 175)

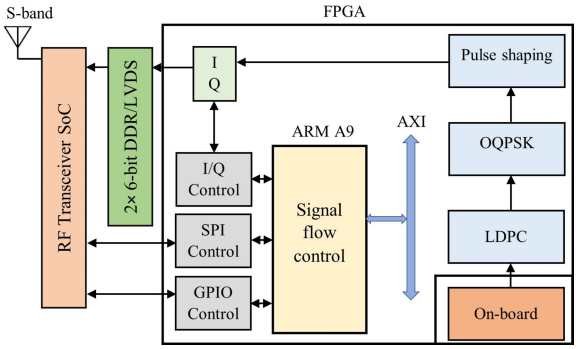

FIGURE 5. Architecture of the SDR transmitter [59].

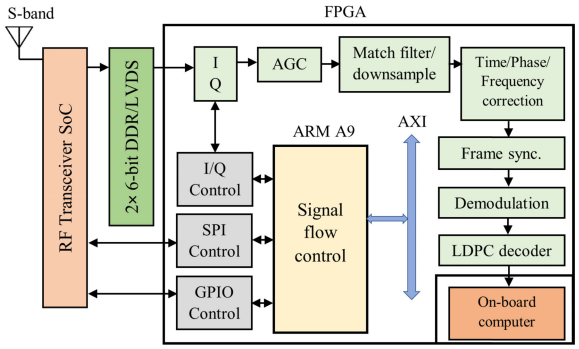

FIGURE 6. Architecture of the SDR receiver [59].

channel coding [59]. There were already previous ISC systems for small satellites such as [60], [61], and [62] but they had considerable limitations. For example, [60] had a high power consumption to achieve a reasonably low bit error rate (BER) and [61] required around 50 iterations in the LDPC decoder to achieve acceptable error correction. Due to the use of OQPSK modulation in [59], an extra 0 bit is added to the code resulting in a code length of 256 bits. LDPC is widely used because its capacity can approach the Shannon capacity limit and so for the same BER, the transmission power can be reduced [59]. A dual-diagonal matrix (a special form of the conventional parity check matrix) is used to obtain the codeword. The advantage of using this dual-diagonal format over the traditional one is that the number of computations needed in the encoding process is reduced from $(n^2 - k^2)/2$ to $(k + 2)(n - k)$ [59]. Also, the number of "XOR" operations needed is reduced saving hardware resources. Reference [59] proposes two versions of this encoding algorithm. The improved version requires even lower number of "XOR" operations resulting in more efficient utilization of hardware resources. Although the improved algorithm significantly reduces hardware utilization, the original algorithm provides higher throughput due to its parallel use of $(n - k)$ groups of "XOR" gates; generates $(n - k)$ parity check bits simultaneously. Fig. 5 illustrates the SDR architecture of the transmitter. A "Zynq 7020" FPGA was used for baseband processing to generate the different baseband signals. The FPGA is responsible for all baseband functions: LDPC encoding, OQPSK, and pulse shaping. In more detail, the data bits are first generated by the PC then sent through an Ethernet interface to the FPGA which performs LDPC encoding on them and maps the coded bits into OQPSK symbols to finally go through a square root raised cosine filter for pulse shaping [59]. On the RF front end, the pulse shaped signals are shifted in frequency by a 2.4 GHz carrier and are then transmitted [59].

Fig. 6 shows the SDR architecture of the receiver, which shares the same structure with the transmitter. In this case, the RF signal is down-converted to a baseband signal by the transceiver and then sent to the FPGA to perform baseband processing: automatic gain control (AGC), matched filtering, demodulation, decoding, and other functions. It was demonstrated that decoding with 50 iterations had almost the same performance as decoding with 20 iterations and only improves the performance by 0.1 dB at BER of 10^{-6} than decoding with 10 iterations [59]. Thus, with only 10 iterations the LDPC decoder can achieve very efficient error correction. The transmitter had a power consumption of 2.1 W while the receiver had a power consumption of 3.2 W [59]. Since the receiver is performing more computationally intensive tasks it had higher power consumption, especially that the transmitted power was quite low given that the transmitter and receiver were only separated by 2 m in the experimental test [59]. The data rate tested in the experimental setup was 122.88 kbps [59]. Although the data rate tested is low, supposedly it could reach up to 28 Mbps [59]. The main features of this design are its efficient LDPC algorithms, high code rate, and least E_b/N_0 at a BER of 10^{-6}.

One of the most recent custom SDR systems for CubeSats is that of UOW (University of Wollongong) CubeSat [32]. The aim of the UOW 3U CubeSat is to be able to transmit images from the satellite in the period of one pass over the ground station (60 seconds) while having an adaptive and on-flight reconfigurable communication system [32], [63]. For a maximum image size of 3 MB, the required data rate would be about 0.42 Mbps. The SDR architecture is divided into digital and analog domain where the analog domain consists of an Analog Front End (AFE), transceiver, and RF front end. The SDR follows the architecture of a Zero-Intermediate-Frequency (ZIF) transceiver where there is no Intermediate Frequency (IF) stage in the communication system [63]. This results in a reduction of the hardware components needed and thus a highly integrated transceiver. The digital baseband signal processing functions are performed using a Cyclone IV E FPGA from Altera [32]. 16-QAM modulation is used to provide high modulation efficiency. This requires the use of two ADCs and two DACs; to operate on the in-phase component and out-of-phase component of the QAM signal simultaneously. Fig. 7 illustrates the different baseband functions performed by the FPGA. The MAX19713 is used for the AFE stage because it incorporates both a pair of 10-bit DAC and a pair of 10-bit ADC into a single device

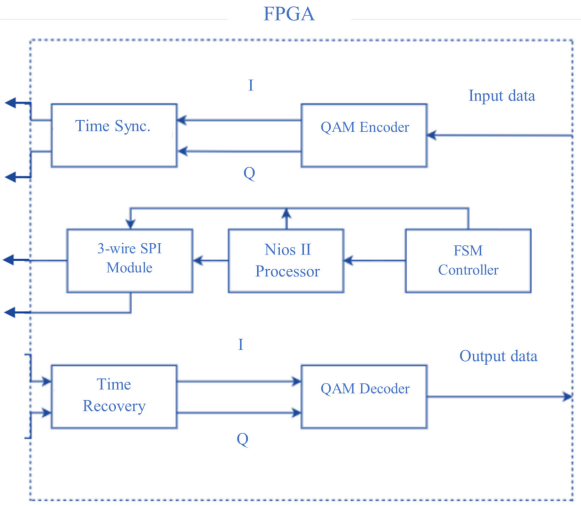

FIGURE 7. Baseband architecture of UOW CubeSat SDR [63].

thus saving space without compromising the performance. The device only consumes 91.8 mW at its full speed sample conversion rate of 45 MSps [63]. Using 16-QAM and three samples per each symbol with the MAX19713 device makes the maximum achievable data rate of the system 60 Mbps. Although this data rate is significantly greater than the minimum data rate needed for image transmission, it is not the actual data rate of the system since this depends on the execution speed of the other blocks as well. Since this SDR operates in a half-duplex scheme, a limitation arising due to the chosen transceiver, only the transmit path or the receive path operates at a given time. Since the received signal by the CubeSat from the ground station can be as low as -80 dBm [64], a Low Noise Amplifier (LNA) is used at the receiver side to increase the SNR and minimize the added noise figure (NF). The chosen LNA has a gain of 13 dB and a very small NF of 0.85 dB at the carrier frequency [32]. The SDR has a power consumption of 0.4 W in the reception mode and 0.6 W in the transmission mode with an additional 2 W for the power amplifier so a total 2.6 W in the transmission mode [32], [63]. However, to optimize the power consumption of the system, the SDR has four operation states that will cycle through as it orbits the Earth. These states are shutdown, standby, receive, and transmit. The FPGA controls the operation state based on the position of the CubeSat in its orbit. It was found that the power consumption in the standby mode is 0.2 W while it is 0.03 W in the shutdown mode [64].

It was found that as AeroCube (Aerospace Corporation CubeSat) travels in its orbit, the SNR can change by more than 20 dB [65]. Consequently, adaptive coding and modulation (ACM) is employed in this system to track the link SNR value and optimize the data rate accordingly by changing the modulation and coding schemes used. The modulation schemes used in this design are BPSK and QPSK. Root raised cosine is used for pulse shaping and Turbo rate 1/4, 1/2 are used for channel coding [66]. Using ACM over fixed modulation and coding schemes has the potential to more than double the average throughput of the SDR [65]. The frequency used by AeroCube is 915 MHz which lies in the UHF band. The developed SDR had a power consumption of 2.5 W in the transmission mode when transmitting a signal of 1 W, while the power consumption in the receive mode was 1.2 W [65]. To reduce the power consumption, the SDR is normally turned off and every 16 seconds it checks whether the ground station is attempting to establish a communication link [67]. In case a communication link is detected, the system will need 3 seconds to boot-up [65]. The data rate of this system is variable depending on the modulation and coding schemes used but based on the data and testing results presented in [65] it is around 1 Mbps.

B. COMMERCIAL SDRs

Several CubeSat transceivers are based on commercially available SDR platforms. Such platforms combine all the necessary hardware components (baseband and RF) to implement a completely functional SDR system that can be programmed and optimized to be used for a specific application [68], [69]. Examples of some widely used commercial SDRs are USRP E310, LimeSDR, SODA, and Iris. A comprehensive review of commercial SDR platforms can be found in [70] and [71]. While [70] focuses on the SDRs' architectures and features of each type of SDR platform, [71] is a practical guide for utilizing these platforms and their supporting software packages.

3CAT-2 is a 6U CubeSat that aims to demonstrate global navigation satellite system reflectometry (GNSS-R) by generating an observable called delay-Doppler maps [72]. 3CAT-2 was launched in 2016 [73] but is currently inactive since its lifetime has ended and because newer satellites (3CAT-3 and 3CAT-4) are currently in development for launch [74], [75], [76], [77]. Although the satellites have different missions, their underlying architecture, which was first developed for 3CAT-2, is almost identical [75], [76], [77]. USRP B210 SDR platform is employed in the CubeSat system. USRP B210 features a Xilinx FPGA, two transmitters and two receivers, fully coherent 2×2 MIMO (Multiple-Input Multiple-Output), and ADC/ DAC [72], [78]. In order to enable two simultaneous receiving channels, which is required for the scientific payload, the SDR is used in dual-receiver mode. Downlink is carried over the S-band at 2100 MHz and the VHF band at 145.995 MHz while uplink is carried over the UHF band at 437.940 MHz [72]. Other frequencies are used for collecting the data in integration with the scientific payload structure which has its own antennas. Different modulation schemes and data rates are implemented in each of the used communication bands. The UHF band (uplink) employs AFSK modulation and has a data rate of 1.2 kbps [74]. Both the VHF and S-band (downlink) are modulated using BPSK with a data rate of 9.6 kbps over the VHF band and 115.2 kbps over the S-band [74].

The VHF and UHF links work together as a full-duplex system for telemetry and command upload while the S-band downlink is used for downloading data from the CubeSat without any uplink commands. LDPC-Staircase is employed for error detection and correction. Data compression is also performed using FAPEC software which can perform lossless compression at a ratio of 1.5 and lossy compression up to a ratio of 40 [73]. Based on the detailed link budget and power consumption data, the estimated power consumption of the CubeSat transceiver is around 1.35 W. It is worth noting that 3CAT-3 transceiver, which has different RF and antenna structure, has a much higher power consumption of 11 W for a slightly improved data rate of 0.5 Mbps [75].

[79] proposed a K/Ka-band receiver that is suitable for deep space exploration missions based on off-the-shelf components [79]. The receiver is designed to be compatible with CubeSats or constellations of CubeSats that receive transmitted signals from the ground or from each other. Besides the RF and baseband frequencies processing, the proposed receiver has intermediate frequency (IF) processing functions at 3.7 GHz [79]. Therefore, the RF front end consists of an isolator, bandpass filter, two LNAs, and an image rejection filter. Then the signal is converted to the IF for further filtering and variable gain amplification. Finally, the IF signal is converted into a baseband signal and all baseband processing is performed on the commercial FPGA-based SDR platform. The SDR platform performs the demodulation of the QPSK signal (at IF) as well as the decoding and error correction based on the selected protocol which is DVB-S2 [79].

The SDR receiver is equipped with additional digital features which are autonomous Doppler shift compensation, autonomous handover between the different base stations, and autonomous determination of the uplink signal characteristics [79]. Regarding the handover, it should be clarified that the SDR receiver itself does not perform handover. In fact, it cannot control or initiate the handover. However, it should be able to detect when the Earth base stations perform handovers. This can be realized in two ways: hard handover and soft handover. First, during the handover process, two base stations transmit the same signal simultaneously. In hard handover, the receiver separately detects the two signals and selects the most powerful one based on the link quality. In soft handover, the receiver jointly detects the two signals and combines them after Doppler correction. But soft handover is more complex as it requires special preamble or a cyclic prefix and additional processing at the receiver [79]. The RF signal has a central frequency of 28.650 GHz, bandwidth of 50 MHz, and roll-off factor of 0.25 [79]. The receiver is able to handle received signals with a data rate up to 80 Mbps [79]. However, since this design is only limited to an SDR receiver, the actual data rate of the complete communication system is determined by the ground stations rather than the CubeSat but, in any case, is limited to 80 Mbps. The total power consumption of the receiver is 8 W divided on the different subsystems as follows: 2.48 W consumed by the Ka-band RF front end, 2 W consumed by the IF SDR processing, 3 W consumed by the FPGA (baseband processing) and CPU, and 0.5 W dissipated by the power supply [79].

Cadet radio was developed in 2011 for the dynamic ionosphere 1.5 U CubeSat experiment, which consisted of two CubeSats communicating with two ground stations [80], [81]. Cadet was completely implemented using power efficient COTS components. The downlink is carried over 460- 470 MHz while the uplink is carried over the 450 MHz frequency [80]. While the downlink data rate is 3 Mbps or more practically 2.6 Mbps with FEC employed, the uplink data rate is only 9.6 kbps since uplink is only used for the transmit command [80]. The uplink signal is FSK modulated while the downlink signal is OQPSK modulated. The uplink signal is also encrypted using 256-bit AES (Advanced Encryption Standard) [80]. The Cadet SDR has power consumption of 141.6 mW for the receiver, 11298.0 mW for the transmitter (peak), and 30.0 mW consumed by the interface electronics, totaling a power consumption of 11.47 W [80].

C. CUSTOM HARDWARE DESIGNS

Hardware implementation has some advantages over SDR implementation, and based on the application and design, it can offer better performance in terms of power, cost, and data rate. Therefore, it is important to investigate the status of hardware transceivers and their performance in comparison with SDR systems. Although the use of COTS components for CubeSat transceivers is favorable in terms of cost, development time, and design complexity, reliability and efficient performance usually demand custom hardware components.

GeReLEO is a Ka-band satellite modem designed to provide connectivity to LEO satellites, via a data relay, with considerable constraints in mass, size, and power [82]. The Ka-band modem employs channel-efficient ACM with LDPC codes for error correction. Multi-frequency time-division multiple access (MF-TDMA) and multiplexing schemes are employed in the system. The building blocks of the GeReLEO concept are LEO satellites equipped with a GeReLEO modem, a GeReLEO gateway, a GeReLEO network control center, and a data relay payload on-board a GEO satellite [82]. MF-TDMA is used for the data downlink and uplink whereas TDM is used for the low rate telecommand link. One LEO satellite is serviced at a given timeslot over several frequency channels. The duration of the timeslot is determined based on the visibility time of the satellite. The GeReLEO consists of a physical layer (PL) that generates the waveforms and a data link layer (DLL) that controls the time and frequency resources access. The GeReLEO transmission scheme is the key element for making the modem energy efficient, a limited complexity FPGA is used to control the processing of the system [82]. The modem supports 12 different modulation and coding schemes based on LDPC

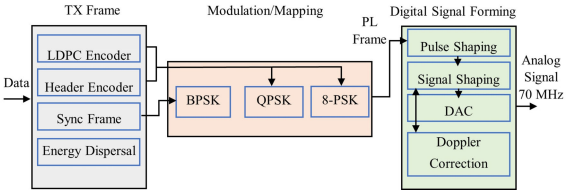

FIGURE 8. Baseband architecture of the GeReLEO transmitter [82].

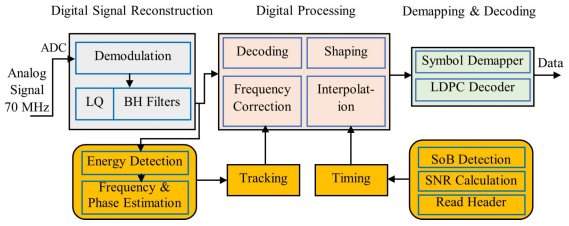

FIGURE 9. Baseband architecture of the GeReLEO receiver [82].

FEC and QPSK or 8-PSK modulation. Furthermore, the modem has two codeword lengths: 9216 bit for the high-rate link and 2304 bit for the low-rate link [82]. The transmitted signal is a series of PL data frames where each sequence of PL frames starts with a synchronization frame, which consists of a string of alternating BPSK symbols and a code for frame synchronization. Each PL data frame in the sequence starts with a PL signaling header (7 bits) and contains either two QPSK modulated codewords or three 8-PSK modulated codewords [82]. The frame and codeword lengths of the high-rate link signal are four times the length of the low-rate link signal. The type of modulation and coding scheme used is specified using 4 bits in the PL signaling header of each frame [82].

The digital signal processing functions as well as the DLL control and resource management are performed on the Zynq device. Thus, GeReLEO modem is a mixed software-hardware radio rather than a completely hardware implemented radio. The baseband architecture of the transmitter consists of three blocks as illustrated in Fig. 8. The first block is responsible for generating the header and data frames, the synchronization frame, and performing the LDPC encoding. The LDPC code rate is a variable parameter varying between 0.25 to 0.78 depending on the quality of the transmission link, and so it is set by the transmitting scheme. This block also performs energy dispersal over the frames to have a uniform energy distribution. The second block is responsible for the modulation: BPSK for the Sync frame and QPSK or 8-PSK for the data frame, depending on the link quality as determined by the transmission control software. It also combines the frame components into the PL frames according to the previously described structure. The third block handles signal shaping and generation. It performs digital pulse shaping with a roll-off factor of 0.35 then converts the signal to the IF and performs Doppler correction according to the calculated Doppler shift.

On the receiver side, the baseband architecture also consists of three main blocks as illustrated in Fig. 9. The quality of the transmission channel is evaluated using signal/noise estimation performed on the header symbols. The Ka-band carrier frequency used for transmission is 25.995 GHz and 23.040 GHz for reception, with a bandwidth of 36 MHz [82]. GeReLEO can achieve a maximum data rate of 1 Mbps in the low-rate link and a maximum data rate of 16 Mbps in the high-rate link [82]. The actual data rate in a given scenario depends on the selected code rate. Although GeReLEO radio was not tested using the actual satellite configuration proposed, an extensive testing procedure that simulates the actual configuration was developed to test the performance of the system. GeReLEO modem has a substantially high power consumption in 1U CubeSat power terms. Its digital board consumes 6 W, its DC-DC converter consumes another 6 W, and its RF front end consumes about 9 W totaling a power consumption of 21 W [82].

The Joint Global Multi-Nation Birds Satellite (BIRDS) is a CubeSat project that started with its first-generation constellation of five identical 1U CubeSats (BIRDS-1) in 2015 [83], [84]. BIRDS-1 CubeSats employed two types of modulation with different data rates. AFSK modulation was used for sending control commands at a data rate of 1.2 kbps [84]. While GMSK was used for data uplink and downlink at a rate of 9.6 kbps [84], [85]. The system used the UHF band for data link and the VHF band for the control line. In BIRDS-2, the VHF and UHF bands are both used for data link using a commercial RF transceiver that handles APRS (Automatic Packet Reporting System) packets [86], [87]. Any user that can handle APRS packets is able to receive transmitted signals from the CubeSats. The UHF band is used for data downlink whereas the VHF band is used for data uplink. BIRDS-2 used the same modulation scheme (GMSK) and data rate (9.6 kbps) as BIRDS-1 for both uplink and downlink [88]. However, BIRDS-2 used deployable monopole antennas [89], instead of the patch antenna used in BIRDS-1. This transition to monopole antennas was made because the gain provided by the patch antennas was insufficient. Also, monopole antennas are easier to deploy and have omnidirectional radiation pattern. BIRDS-2 faced many difficulties in its communication link that required major developments in BIRDS-3 communication system. Firstly, BIRDS-3 CubeSat uses a dipole antenna operating at the UHF band. Moreover, several other improvements on the RF front end were developed such as improvement of the ground plane and EMI (electromagnetic interference) countermeasures [83]. Also, the antenna gain was increased by 4 dB by using circular polarized antenna instead of linear polarized antenna [83]. Overall, BIRDS-3 was able to achieve a link budget improvement of 17.7 dB compared to BIRDS-2. On the baseband side, the uplink command size was decreased from 33 bytes to 14 bytes and the uplink speed was decreased from 9.6 kbps to 4.8 kbps since the amount of uplink data needed has been decreased and so

slower rate can be used to increase the uplink success rate. BIRDS-3 CubeSat has a transmission power of 80.3 mW, after considering the antenna gain [83]. Based on the given power supply description, the power consumption of the transceiver is around 3 W.

Palo proposed a high-rate X-band transmitter suitable for CubeSat applications [90]. The proposed transmitter operates at a frequency of 8.380 GHz and has a transmitted signal power of 1 W from an omnidirectional antenna [90]. The X-band transmitter used has a power efficiency between 20-25% [90]. The transmitter has a basic baseband architecture that consists of OQPSK modulation and has two options for FEC, which are LDPC and convolutional encoding. All other signal processing functions are performed in the RF front end stage. The proposed transmitter is able to achieve a data rate of 12.5 Mbps [90], however, the system has not yet been demonstrated in actual space environment and its testing was limited to the lab. Given that the X-band transmitter has a power consumption of 5 W and the baseband components have a power consumption between 1- 2 W, the total power consumption of the CubeSat transmitter is about 6.5 W. However, this figure does not take into account the receiver's power consumption.

Phoenix CubeSat is designed using some COTS components and several custom designed boards developed by the Phoenix team. Phoenix has three operation modes which are idle, science, and safe mode [91]. The idle mode accounts for around 90% of the orbital period of the satellite, during which the satellite is in low-power mode only transmitting and receiving telemetry commands such as the temperature and power status of the satellite [91]. In the science mode, the CubeSat performs its scientific payload operations such as thermal image collection and calibration [91]. In this mode as well the collected images are sent to the base station. Complete image downlink can require several passes over the ground station in order to transmit all the collected data. The safe mode is an emergency mode that is declared when a fault is detected in the CubeSat so that the CubeSat operation is stopped until the fault is fixed. Both uplink and downlink are carried over the UHF band at 437.35 MHz [91]. The system employs GMSK modulation and uses the AX.25 data link layer protocol with HDLC (High-Level Data Link Control) encapsulation [91]. Additionally, cyclic redundancy check (CRC) is used for error detection and correction. Moreover, a custom packetization method was developed to help in recovering large files by the team. Before transmission, any file with a size greater than 256 bytes is broken into smaller files which are then transmitted as individual packets and reassembled into a single file in the ground station. In case any packet is not received, it is re-requested from the CubeSat until the entire file is successfully reconstructed. The communication system also utilizes an encryption scheme that is incorporated into all uplink command signals. The command signals are encrypted by a rotating cipher key that uses a simple substitution scheme [91]. The encryption process is only applied to the uplink signals from the base station. The downlink signals from the satellite which communicate the image data and all associated telemetry are not encrypted because they are not considered proprietary [91]. The communication system has a low data rate of about 10 kbps [91]. The average power generated by the CubeSat's body-mounted solar panels during an orbit is around 6 W [91]. However, during Sun facing, the solar panels can generate up to 14 W [91]. Based on the simulation and testing of the CubeSat's power budget, the average generated power is sufficient to meet the average power consumption demand of the CubeSat. However, the exact power consumption of the communication system is not measured.

D. COMMERCIAL HARDWARE DESIGNS

Planet is an Earth imaging company that developed several CubeSat and small satellite constellations to image the whole Earth daily and identify environmental changes and trends. Planet operates the world's largest fleet of commercial remote sensing satellites [92]. In total, there are more than 24 Flocks, with more than 350 satellites, that have been launched by the company [93], [94]. The average mass of the 3U Dove CubeSat is 4.7 kg [95]. Dove CubeSat is purely designed using COTS components that are integrated by the Planet team using their own circuit boards [96]. Dove has a simple power conservative operation scheme; it starts by imaging the intended region and locally saving the images. Then, when the CubeSat is above the ground station, it automatically turns on its transmitter and downlinks the images to the ground station. After the transmission process is completed, the transmitter is turned off again [97]. The operation of Dove is inclined towards using on-board fully automated systems for commissioning and operating the satellites rather than waiting for periodical commands from the ground station. Manual commands are only used in case of anomalies or need of making system updates or corrections.

The most sophisticated transceiver was designed for the 3U Build 14 Dove (B14) CubeSat, which was launched in November 2018 [98]. Dove B14 is the world's fastest X-band LEO satellite with an on-orbit maximum data rate of 1.674 Gbps [98], [99]. The satellite is able to download up to 85 GB of image data in one ground station pass. Although the Ka-band has much more available bandwidth than the X-band, it has higher path loss through the atmosphere and suffers from limited availability of COTS components such as mixers and filters compared to the X-band [99]. Hence, Dove B14 employed the X-band for its high-speed radio, named HSD2 radio, since the design is completely based on COTS components. The radio consists of a CPU for control and processing, an SSD (solid state drive) for local data storage, six DVB-S2 modulation cores each running at a baud rate of 76.8 Msps for modulation and FEC, an FPGA for multiplexing the incoming data to the six modulator cores, two X-band transmitters, two antennas, and power amplifiers, filters, etc. [37], [99]. Much of the modulation

complexity is handled by the commercial DVB-S2 cores [37]. The radio operates in the 8025-8400 MHz band and has dual circular polarization antennas that allow for doubling of bandwidth utilization [99]. That is why the radio has two independent transmitters and antennas. For each of the two types of circular polarization, three frequency channels are used simultaneously each with a bandwidth of 96 MHz and channel spacing of 100 MHz [99]. Hence, the use of six DVB-S2 cores as previously mentioned. Each individual channel has approximately a data rate of around 200 Mbps resulting in an average combined data rate of about 1.3 Gbps [99]. On the baseband side, adaptive modulation and channel coding is employed according to the DVB-S2 standard with modulation options of QPSK, 8-PSK, 16-APSK, and 32-APSK [99]. Regarding the channel coding, FEC based on LDPC concatenated with BCH is employed using code rates between 1/4 to 9/10 [99]. The DVB-S2 standard was selected due to the wide variety of options for the COTS components that can be used to realize this standard [37]. The downlink is carried over the X-band with a maximum demonstrated data rate of 1674 Mbps [99]. On the other hand, the uplink is carried over the S-band at a data rate of 256 kbps [99]. On the ground side, there are five ground stations at five different locations with a total of 15 antennas [99]. Although the Dove B14 communication system has a very compact size of only 0.25 U, it has an exceptionally high power consumption of 50 W [99]. Such a high power consumption is expected given the intensive complexity of the system; six modulator cores, two transmitters, and two antennas all working simultaneously in addition to the FPGA and CPU. Thus, the very high data rate of the system comes at the expense of increased complexity and very high power consumption.

Another notable commercial hardware system is that of Corvus-BC CubeSat. Corvus-BC is a 6U CubeSat developed for multi-spectral Earth imaging [100]. The 1U communication system of Corvus-BC operates at a central frequency of 26.8 GHz with a bandwidth of 86.4 MHz in the Ka-band [100]. The Ka-band radio employs the DVB-S2 link-layer protocol and is able to operate all of the 28 different modulation and coding schemes supported by the protocol [100]. The 28 different options are based on the valid combinations between one of the four modulation schemes, which are QPSK, 8-PSK, 16-APSK, and 32-APSK, and one of the 12 possible coding rates (1/4 - 9/10) of LDPC concatenated with BCH [35]. The maximum data rate achievable by this radio is 320.6 Mbps [100]. However, the average on-orbit data rate is about 185 Mbps [100]. The power consumption of the transceiver is around 24 W [101].

One of the advantages of using the Ka-band is the smaller antenna size for both the transmitter and receiver. For instance, to achieve the same data rate over the X-band, the diameter of the ground station's dish has to be more than twice the diameter of the Ka-band dish which is about 2.8 m [100]. Larger dishes require considerably higher development and operation costs. Moreover, the data rates achieved on the Ka-band, and the X-band as well, demonstrate these band's ability to achieve much higher data rates than the near term proposed CubeSat optical communication systems. In fact, the X-band and Ka-band CubeSats achieved higher data rates compared to CubeSats using optical communication bands, and without the enormous technical obstacles that face these optical communication systems [100]. For instance, NASA's Optical Communications and Sensors Demonstration (OCSD) program was able to establish a CubeSat optical communication link at a maximum data rate of 100 Mbps using a 1.5U 2.3 kg CubeSat [102]. Although the achieved data rate is higher than most reviewed systems, the last two X-band and Ka-band designs achieved much higher data rates. Consequently, given the additional complexities and shortcomings of optical bands, such as the heavy dependence of optical connectivity on the cloud coverage, the X-band and Ka-band have much better potential in achieving very high data rate uninterrupted communication links than optical bands.

There are some older CubeSat transceivers that had some noticeable features such as [103], [104], [105], [106], [107], and [108]. For example, [108] was able to implement both AFSK and GMSK modulation schemes on a DSP connected to a VHF transceiver which had a transmission power consumption of 1 W for a data rate of 1.2 kbps for the AFSK modem and 4.8 kbps for the GMSK modem. Some of these older CubeSat designs are reviewed in [109]. The majority of those systems had data rates between 1- 10 kbps for a power consumption between 0.5- 1 W [109].

IV. PERFORMANCE EVALUATION

A. COMPARISON BETWEEN THE REVIEWED SYSTEMS

Table 2 provides a critical summary of the reviewed systems compared in terms of their design approach, mission objective, modulation and coding schemes, practically demonstrated data rate in Mbps, power consumption in W, and the frequency bands used. Out of the 14 reviewed systems, five of them used the S-band, four used the VHF/UHF bands, three used the Ka-band, and only two used the X-band.

Fig. 10 displays the data rate and corresponding power consumption of each of the reviewed systems illustrated by design category. The y-axis, which represents the data rate in kbps, has a logarithmic scale to accommodate the orders of magnitude variation between the different data rates. Only six of the reviewed systems had a power consumption less than 5 W, ten systems had a power consumption less than 10 W, while four systems had power consumption above 10 W. For the data rate, only two systems had a data rate above 100 Mbps, four systems had a data rate between 10- 100 Mbps, two systems had a data rate around 1 Mbps, and six systems had a data rate much less than 1 Mbps. It can be noted that nine systems employ QPSK, either alone or with other types of modulation, and eight systems employ LDPC for channel coding. However, only two systems employed

TABLE 2. Comparison between the reviewed CubeSat communication systems.

System	Design Category	Mission Objective	Modulation Scheme	Coding Scheme	Data Rate (Mbps)	Power Consumption (W)	Bandwidth
PULSAR [27]	Custom SDR	Technology demonstration.	QPSK.	LDPC, convolutional, and Reed-Solomon.	5- 10	0.5- 1	S-band.
Maheshwarapp [55]	Custom SDR	Multi-CubeSat signal reception.	BPSK.	Viterbi and Reed-Solomon.	0.0192	2.709	VHF, UHF, and S-band.
Cai [59]	Custom SDR	CubeSat ISC.	OQPSK.	LDPC.	0.12288	5.3	S-band (2.4 GHz).
UOW [63]	Custom SDR	Imaging.	16-QAM.	None.	Not tested	2.6	S-band (2.4 GHz).
AeroCube [65]	Custom SDR	Technology demonstration.	BPSK, QPSK.	Turbo.	1	2.5	UHF (915 MHz).
3CAT-2 [74]	Commercial SDR	Global Navigation Satellite System Reflectometry.	AFSK, BPSK.	LDPC-Staircase.	0.1152	1.35	VHF, UHF, and S-band.
Alimenti [79]	Commercial SDR	Deep Space Exploration.	QPSK.	LDPC concatenated with BCH.	Not tested	8	Ka-band.
Cadet [80]	Commercial SDR	Dynamic Ionosphere Experiment.	FSK, OQPSK.	None.	2.6	11.47	UHF.
GeReLEO [82]	Custom Hardware	Provide LEO inter-satellite links.	QPSK, 8-PSK.	LDPC.	16	21	Ka-band.
BIRDS-3 [83]	Custom Hardware	Imaging & Technology demonstration.	GMSK.	None.	0.01	3	UHF (437 MHz).
Palo [90]	Custom Hardware	Technology demonstration.	OQPSK.	LDPC and convolutional.	12.5	6.5	X-band (8.380 GHz).
Phoenix [91]	Custom Hardware	Infrared remote sensing.	GMSK.	CRC.	0.01	6	UHF (437 MHz).
Dove B14 [99]	Commercial Hardware	Earth imaging.	QPSK, 8-PSK, 16-APSK, 32-APSK.	LDPC concatenated with BCH.	1674	50	S-band and X-band.
Corvus-BC [100]	Commercial Hardware	Multi-spectral Earth imaging.	QPSK, 8-PSK, 16-APSK, 32-APSK.	LDPC concatenated with BCH.	320.6	24	Ka-band (26.8 GHz).

some kind of encryption or source encoding scheme in their communication system. To conclude this comparison, it can be noted that more than half of the reviewed designs were based on SDR, specifically eight systems, while six systems were based on the more conventional hardware radio design approach.

B. PERFORMANCE OF CUSTOM SDR SYSTEMS

Although the PULSAR SDR has the lowest power consumption among all reviewed systems and the highest data rate among all custom SDR systems, it did not go through extensive testing stages to demonstrate its BER performance in the orbit environment. The FPGA-based design demonstrated very low power consumption of 1 W for a data rate of 10 Mbps but its performance in terms of BER has not been tested. However, given that the SDR utilizes various types of error correction schemes and NEN compatible packetization, it is expected that the system has acceptable communication quality. On the other hand, Maheshwarapp SDR has undergone extensive simulation, laboratory, and practical CubeSat communication testing stages. The system was tested as a ground transceiver using two different practical testbeds with both FUNcube-1 CubeSat and ESEO microsatellite and it successfully demonstrated reliable multi-CubeSat communication at a data rate of 19.2 kbps. Although the demonstrated data rate is very low with respect to the system's power consumption of 2.7 W, the SDR is not meant to provide high speed CubeSat downlink but to provide simultaneous multi-CubeSat signal reception capability. Consequently, the system has two separate communication chains working simultaneously over

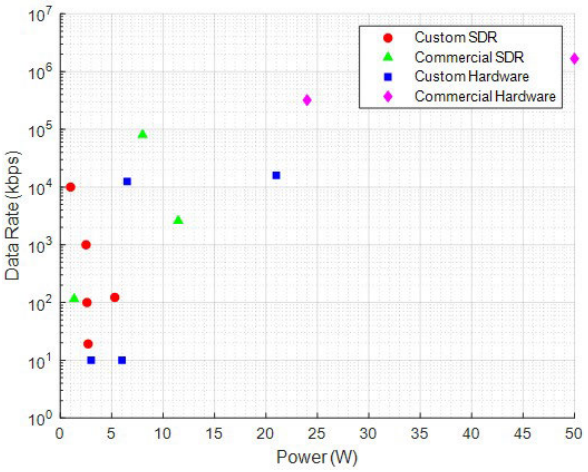

FIGURE 10. Power consumption versus data rate of the reviewed systems by category.

the S-band for inter-satellite link and over the VHF/UHF band for uplink/downlink. This justifies the high power consumption to the low data rate of this system.

Cai SDR has the highest power consumption among all custom SDR systems. Moreover, its demonstration was only limited to in-lab testing and did not undergo actual space testing. The most notable feature of this design is the improved algorithm of LDPC that was developed and implemented for the channel coding of this system resulting in very efficient utilization of the FPGA resources. Moreover, with this improved LDPC algorithm the achieved BER (10^{-6}) was much lower than other systems for the same number of decoding iterations (20) and for the same SNR (4.9 dB). Thus, Cai SDR has superior BER performance compared to most other systems. Although it is claimed that the SDR can achieve a data rate of up to 28 Mbps, this data rate has not been demonstrated in practical testing. Although UOW SDR was tested in-lab, the testing lacked several important criteria. Firstly, the SDR was tested either as a transmitter or as a receiver at a given time. Therefore, there was no complete communication chain testing of the developed SDR. As a result, the actual data rate that the system is capable of was not determined. Instead, only the maximum possible data rate limit (60 Mbps) allowed by the system's components is known. Although the actual data rate of this SDR was not determined, it is expected to be above 100 kbps based on the system's specifications and results from similar systems. Secondly, the testing was merely limited to verifying the functionality of the individual blocks, the overall functionality of the SDR, and the power consumption, rather than to test the practical performance of the system under realistic conditions. Thirdly, the testing was completely performed in-lab and no testing was performed using either existing CubeSats or UOW CubeSat itself.In contrast, AeroCube SDR, which had nearly the same power consumption as UOW SDR, was able to successfully implement FEC codes and even utilize ACM to change the modulation and channel coding schemes based on the channel conditions and in-orbit position. Moreover, AeroCube SDR demonstrated a data rate of around 1 Mbps based on in-orbit results. Although the exact BER performance of the system is not described, it is expected to have acceptable BER based on the successful results of the CubeSat.

C. PERFORMANCE OF COMMERCIAL SDR SYSTEMS

3CAT-2 SDR had both the lowest data rate and power consumption among the reviewed systems. A distinguishing feature of 3CAT-2 is that its SDR platform (USRP B210) employs a 2×2 MIMO. Therefore, the SDR is able to support two simultaneous transmitting and receiving channels. The SDR was successfully tested on board the 3CAT-2 CubeSat, providing a reliable 115.2 kbps downlink data rate over the S-band at an approximate 1.35 W power consumption. On the other hand, Alimenti SDR had a noticeably high power consumption for a receiver-only system. Although the Ka-band receiver is capable of handling up to 80 Mbps data rate, this has not been demonstrated in practical CubeSat deployment. Furthermore, due to the considerably high power consumption of the receiver-only system, around 8 W, it is very challenging to be used for typical CubeSat applications. Cadet SDR had the highest power consumption among all reviewed SDR systems. The SDR required a power of 11.47 W to achieve a data rate of 2.6 Mbps. A distinguishing feature of Cadet system is its use of encryption for uplink signals. All the uplink ground commands are encrypted using 256-bit AES and are decrypted by the CubeSat receiver. This ensures that the CubeSat does not respond to third-party commands. Although the exact BER performance of the SDR is not mentioned in the work, successful communication with the CubeSat was achieved demonstrating the reliability and performance of the system.

D. PERFORMANCE OF CUSTOM HARDWARE SYSTEMS

For the performance of custom hardware systems, it can be noticed that both BIRDS-3 and Phoenix systems had similar characteristics. Both systems employed the same frequency over the UHF band, both had a low data rate of 10 kbps, and they both employed GMSK modulation. However, Phoenix used a rotating cipher for encrypting all their uplink command signals. Due to the additional features of Phoenix system, it had higher power consumption than BIRDS-3 system. Nevertheless, BIRDS-3 had a more developed RF front end compared to Phoenix. For instance, while Phoenix used a simple omnidirectional antenna, BIRDS-3 used a circularly polarized dipole antenna with special EMI countermeasures. Although BIRDS-3 has a very basic baseband system, it was able to accomplish its mission at its very low data rate. On the other hand, Phoenix failed to achieve its scientific mission due to an unexpected fault after its deployment, but it successfully demonstrated two-way communication according to the expected performance.

GeReLEO system had both the highest data rate and power consumption among the custom hardware systems.

The design was not completely hardware-based but used SDR for several functions; hardware-software co-design. A unique feature of GeReLEO system is that it used multiple access techniques, which is not common among the reviewed systems. It employed MF-TDMA for its data downlink/uplink and TDM for its telecommand link. Moreover, the system passed through a rigorous testing stage that simulated the practical channel conditions for the proposed CubeSat configuration. The system demonstrated, in implementation, the ability to provide a high-quality link with a BER of around 10^{-7} for an SNR of roughly 5 dB using QPSK with a code rate of 2/3. Given that GeReLEO is the only custom hardware system that operates over the Ka-band and has the highest data rate (16 Mbps) among custom hardware systems, it is expected that it has the highest power consumption (21 W), greatest mass (2.4 kg), and largest dimensions (20.3 cm × 20.0 cm × 7.7 cm) among the reviewed custom hardware systems.

Finally, Palo design consisted of a transmitter-only system. The system used a simple omnidirectional antenna with a transmitter power efficiency of roughly 25%. Although the proposed transmitter can achieve a maximum data rate of 12.5 Mbps, its demonstration was limited to in-lab experiments. Furthermore, the implementation and testing only focused on the performance of the X-band transmitter, without enough consideration to the corresponding X-band receiver. Hence, it is difficult to evaluate the proposed system in terms of actual data rate, BER reliability, and total power consumption.

E. PERFORMANCE OF COMMERCIAL HARDWARE SYSTEMS

Commercial hardware systems had by far the highest data rates among all reviewed systems. Dove B14 demonstrated an in-orbit data rate of 1.674 Gbps making it the world's fastest X-band LEO satellite. This extremely high data rate comes at the expense of the very high, 50 W, power consumption, large mass of 4.7 kg, and increased complexity of the system. Dove B14 was able to achieve such an exceptionally high data rate due to several reasons. Firstly, it had two antennas radiating simultaneously at two different polarizations (right-handed and left-handed circular polarization) and employed three frequency channels for each polarization. Thus, six simultaneous frequency channels are being used by the CubeSat for downlinking the data. Secondly, the system had six DVB-S2 modulation cores each operating at a baud rate of 76.8 Msps, simultaneously. Hence, each channel has its own high-speed modulation core. Thirdly, the system has a CPU dedicated to signal control and processing. Fourthly, the system has an FPGA dedicated to multiplexing the incoming data to the six modulators. Consequently, the transceiver has superior processing power, high utilization of the available bandwidth resources, high gain, and employs different polarizations. Both Dove B14 and Corvus-BC transceivers employed the DVB-S2 standard. So, they have exactly the same modulation and channel coding options.

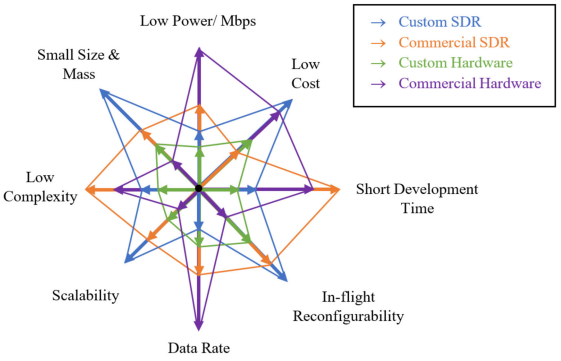

FIGURE 11. Qualitative comparison between the features of each CubeSat communication subsystem design approach.

However, while Dove B14 works over the S-band (uplink) and X-band (downlink), Corvus-BC works over the Ka-band at a much higher frequency. This has the key advantage of requiring smaller antenna size thus making the system more compact.

V. DISCUSSION

A. FEATURES AND LIMITATIONS OF EACH DESIGN APPROACH

To compare the general features of each of the four design approaches, Fig. 11 has been developed to provide a visual overview of how the different design approaches perform under eight different metrics. Under each metric, the performance of the approach is represented by the length of its arrow, where longer arrows indicate better performance. The metrics are the average consumed power over the achieved data rate (average W per Mbps), the typical development cost, the required development time, the hardware and software complexity of the system, and the size and mass of the system. Longer arrows under these metrics indicate lower consumed power for a given data rate, lower cost, shorter development time, lower complexity, and smaller size/mass, hence better performance. The other set of metrics are the average demonstrated data rate, the in-flight reconfigurability, and the capability of the system to be easily upgraded or scaled after deployment. For these metrics, longer arrows indicate higher data rate, better reconfigurability and scalability, and consequently better performance as well. The comparison is directly based on the average performance of the reviewed systems under each design category. Therefore, it reflects the overall features of each of the design approaches for CubeSat communication subsystems.

Custom SDR approach performs fairly well in most metrics. It has the lowest cost of implementation, best in-flight reconfigurability, best scalability, smallest size, moderate complexity, and moderate development time. Its primary limitation is that it has the lowest data rate and has a noticeably high power consumption with respect to the achieved data rate. Commercial SDR systems strongly compete with custom SDRs, they have similar performance

under several metrics such as reconfigurability, scalability, and size. However, they have slightly higher data rates and better power efficiency but at more expensive costs. Moreover, commercial SDRs have the lowest complexity and shortest development time. Commercial hardware systems succeeded in achieving the highest data rates ever achieved using CubeSats and small satellites in general, however, they have the largest size and mass among all systems. Nonetheless, commercial hardware systems demonstrated the lowest power consumption required for achieving a given data rate. On the other hand, both commercial and custom hardware systems have very little capability to be reconfigured or upgraded after deployment. Consequently, they are not as flexible as SDR systems and if a fault were to occur in the system, most likely, it will be very difficult to fix, as actually happened with Phoenix CubeSat. On the other hand, SDR systems can easily be upgraded, reconfigured, and fixed. Hence, they are less likely to fail the mission.

While normally custom hardware systems have smaller sizes and better power efficiency than SDR systems, this is not the case for the reviewed CubeSat systems. This can be traced back to several reasons. Firstly, two of the reviewed custom hardware systems (BIRDS-3 and Phoenix) operated in the UHF band and had a considerably low data rate (10 kbps) for a relatively high power consumption. Secondly, GeReLEO custom hardware system operated at a very high frequency in the Ka-band which largely explains why it had a very high power consumption (21 W) for its achieved data rate of 16 Mbps. Furthermore, GeReLEO transceiver had a large mass of 2.4 kg and large dimensions. This is in contrast with Alimenti commercial SDR system which also operated in the Ka-band but had a much lower power consumption of 8 W and a much smaller mass of 0.6 kg. To summarize, the comparison given in Fig. 11 must be interpreted in the context of this review.

B. CHALLENGES AND FUTURE DIRECTIONS

There are many directions for improving the capabilities of CubeSat communication subsystems to meet the increasing demands of higher data rates at lower costs, lower power, smaller form-factors, and higher flexibility. The improvements include using high frequency bands, better modulation and coding schemes, improved baseband algorithms, use of MIMO and beamforming technologies, employment of multiple access techniques, use of advanced antennas, and use of efficient high-speed processors.

1) HIGH FREQUENCY BANDS

Current and future trends include using higher frequency bands especially the Ka-band. Increasing the system's RF frequency not only increases the data rate, due to the more available bandwidth at higher bands, but also decreases the required antenna size and mass of the transceiver. Due to this relatively recent trend towards using higher frequency bands, about 66 nanosatellites communicate over the Ka-band [13]. It is expected that the number of nanosatellites operating at these high frequency bands will grow rapidly in the future. The transition towards higher bands is mainly driven by the demand for much higher data rates and the fact that low bands are highly congested. The bandwidth available at high frequency bands, such as the Ka-band, is many times larger compared to that available at lower bands and thus the achieved data rate can be many times higher [99]. However, this transition is hindered by the relative lack of energy-efficient COTS components operating at such high frequencies as well as the other challenges that face high-frequency communications such as increased power consumption, significantly higher path loss, and need for much faster processors to handle such high data rates. The Ka-band specifically has much higher attenuation through the atmosphere and higher rain and cloud fade [99]. Although the optical band is a very attractive option as it has practically unlimited available bandwidth, it still faces considerably severe challenges for CubeSat applications such as the very expensive costs, critical dependence of connectivity on cloud coverage, and power efficiency of optical communication systems [99].

2) EFFICIENT MODULATION SCHEMES

Based on analyzing the data from a data-set [110] containing information on 757 CubeSats deployed in orbit, Fig. 12 has been developed to give a statistical insight of the most common CubeSat modulation schemes and antenna types. GMSK was the most widely used modulation scheme followed by BPSK, FSK, QPSK, and AFSK, which all had nearly the same percentage. Most CubeSat transceivers tend to use the aforementioned modulation schemes, especially GMSK and BPSK, due to the complexity of higher order modulation transceivers and the strict limitations on power consumption [111]. BPSK is the one of the most widely used modulation schemes for CubeSats because it is simple to implement and demands the least amount of power to support a given throughput [111]. GMSK is uniquely attractive for its efficient spectral characteristics, although it has worse BER performance compared to BPSK [111].

3) HIGH-GAIN ANTENNAS AND MIMO

Dipole antennas and patch antennas were employed in almost 70% of the deployed CubeSats. The design of more efficient and high-gain antennas is a critical method for improving CubeSat communications. For example, [112] described the design and successful implementation of a high gain S-band slot antenna that significantly increased the gain from 2.52 dBi to 8.8 dBi. Improvements on the antenna design are not just limited to increasing the gain but can extend to decreasing the antenna size, increasing its power efficiency, and use of beam steering techniques if required [112]. Moreover, the use of multiple antennas, which is still not common in CubeSats, to exploit the features of MIMO and beamforming techniques is an important development to increase the data rate and serviceability,

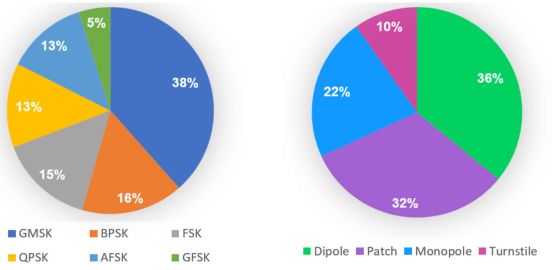

FIGURE 12. Modulation schemes used by 182 CubeSats (left) and antenna type used by 245 CubeSats (right) launched between 2015 – 2018.

especially if we consider mobile ground stations. Such development faces many challenges including power, size, complexity, and need for more powerful energy-efficient processors to execute the various MIMO/beamforming algorithms. Consequently, employing beamforming requires considerable improvements on both the RF and baseband sides.

4) MULTIPLE ACCESS TECHNIQUES

Another aspect of future development is the use of multiple access techniques. Most existing CubeSats do not make use of any multiple access techniques. Multiple access techniques such as OFDM (Orthogonal Frequency Division Multiplexing) increase the efficiency of resource utilization and lead to higher data rates or larger number of serviceable users [113]. The use of multiple access techniques for inter-satellite communication between small satellites was already long proposed, as in [114] and [115]. Reference [116] presented a comparison between various multiple access techniques that can potentially be used to overcome some of the challenges that face inter-satellite communications.

5) IMPROVED CHANNEL CODING ALGORITHMS

On the baseband side, channel coding is an essential block for all reliable CubeSat systems because it substantially reduces the required transmitter power by reducing the SNR requirement for achieving a given bit error rate. Besides employing efficient error correction schemes, developing customized algorithms to implement the encoding and decoding processes is an important factor for designing more efficient systems. Improved channel coding algorithms can greatly reduce the required hardware resources needed to perform encoding/decoding. This results in lower processing power utilization and hence lower power consumption. Moreover, channel coding algorithms can be customized to reduce the number of iterations required to achieve a specific BER at a given SNR or reduce the SNR requirement for a given BER. Furthermore, some algorithms can allow higher data rates than others based on the number of operations required and whether they are performed in series or in parallel. Consequently, developing improved and customized channel coding algorithms is a major way for improving the communication system in terms of efficiency, reliability, power consumption, and data rate. Nevertheless, the literature on CubeSat communication systems does not address this issue in sufficient detail. The majority of existing CubeSats employ existing channel coding algorithms without consideration to customizing or improving them to better suit the specific requirements of CubeSats.

6) ENERGY RESERVE BUDGETING

Of all the challenges facing CubeSat transceivers, the strict limitation on the power consumption is the most severe challenge. The small size of the CubeSat restricts the size of its solar panels and batteries and thus limits the available power and energy resources. There are two approaches to overcome this limitation: maximizing the harnessed solar power and minimizing the systems' power consumption. There are several proposals for increasing the harnessed solar power such as the use of more efficient solar panels, use of deployable panels, and choice of optimum orbit that maximizes the harnessed solar power. When it comes to reducing the consumed power, this decrease should not come at the expense of lower performance. In contrast, the decrease in power should stem from using more efficient components that achieve the same performance at lower power consumption. One of the major aspects for realizing this is the use of FPGAs due to their unique energy-efficient features described previously. Although FPGAs can provide high data processing performance at a reduced power consumption, FPGAs' power demand can still easily exceed CubeSats' power budget. For instance, the radiation tolerant Virtex4QV FPGA family's average power consumption can range from 1.25 W to 12.5 W, while a typical 1U CubeSat power budget ranges from 2 W to 8 W [117]. Even more, the average obtained power using body mounted solar panels on 3U CubeSats is typically less than 10 W [118]. Consequently, it is necessary to develop and employ energy reserve budgets and power-saving operation modes. Reference [117] proposes two energy reserve budgeting scenarios for FPGA-based CubeSats based on the orbital pattern to determine the percentage of orbital time available for FPGA processes that require high power.

7) DEPLOYABLE SOLAR PANELS

There are several methods for increasing the generated solar power, most commonly by using deployable solar panels that are initially folded on the CubeSat sides and extend to their full size once the CubeSat is in orbit. This technology is further improved by designing solar panels that can track the apparent motion of the sun. Reference [118] designed a solar panel system for a 3U CubeSat consisting of two deployable systems made of three solar panels each for a total of six deployed solar panels that can track the sun's apparent motion. The system was able to deliver a maximum power of 50.4 W [118]. More generally, deployable solar panels produce between 160% to 400% more power than body mounted solar panels [119]. There are many deployable

solar panel solutions for 3U CubeSats with total generated power ranging from 22 W to 56 W [120], [121], [122]. Therefore, using deployable solar panels greatly increases the amount of generated power which can be utilized to enable the employment of some of the techniques mentioned before such as beamforming and multiple access. However, it must be noted that these solar panel solutions come at the expense of higher development costs, larger CubeSat mass, and increased complexity. Comparing the typical generated power, even with deployable solar panels, with the reported power consumption of the reviewed communication systems, keeping in mind that there are other systems on the CubeSat that also have high-power requirements, it is evident that there is a definite need for reducing the required power consumption per achieved Mbps that CubeSat transceivers are capable of.

8) INTEGRATED ANTENNA SYSTEMS

One of the main challenges in increasing the efficiency of harnessing solar power in CubeSats is optimizing the utilization of CubeSat sides. CubeSats have limited surface area, which is typically allocated for solar panels. However, there is potential for integrating antenna systems with the solar panels or other payloads to improve overall mission efficiency [123], [124]. By integrating antennas into the surface area of the CubeSat, it becomes possible to simultaneously utilize the limited space for both communication and power generation purposes [125]. This integration eliminates the need for separate dedicated antenna structures, saving valuable space and reducing the overall size and weight of the CubeSat [16]. Integrated antenna systems offer several advantages. Firstly, they enable efficient use of the CubeSat's surface area, maximizing the available space for solar panels while also providing the necessary antenna functionality [123]. This can be particularly valuable for missions that require extensive communication capabilities or have strict power requirements. Moreover, integrating antennas with solar panels or payloads can enhance the pointing accuracy and coverage of the antenna system [126]. By aligning the antenna with the solar panels, it becomes possible to optimize the CubeSat's orientation towards the desired communication target or increase the field of view for better signal reception [126]. Furthermore, this approach can contribute to improved system-level integration and reduced interference between components. By combining the antenna, solar panels, and other payloads into a single integrated structure, potential interference issues and complexity associated with separate components can be minimized [127]. Nonetheless, the integration of antennas with solar panels or other payloads presents new design challenges. These include managing potential electrical and electromagnetic interference, ensuring proper thermal management to avoid overheating, and maintaining the structural integrity of the system [17]. Extensive research and development efforts in the literature explore the feasibility, performance, and practical implementation of integrated antenna systems in CubeSats [16], [128], [129]. This approach has the potential for enhancing the efficiency of CubeSats, enabling improved communication and power generation within the limited available space.

Concrete real-world examples of integrated antenna systems for CubeSats remain relatively limited due to the concept's emerging stage [16], [125], [126]. For instance, within the QB50 project, which aims to establish a constellation of CubeSats for atmospheric research, the CubeSat ''EnduroSat One'' employed integrated patch antennas to enhance its communication capabilities. The CubeSat had embedded patch antennas on its sides and top panels, effectively utilizing its surface for communication and power generation [17]. This dual-purpose integration emphasizes the potential to merge functionalities within the limited spatial borders of CubeSats [128]. Another practical case is TDSat, which incorporates an integrated deployable Yagi-Uda antenna, showcasing the practical integration of an antenna system into the CubeSat's structural framework [16], [129]. While the integration of antenna systems into CubeSats is still evolving, these cases as well as the ongoing research efforts demonstrate the potential of this approach in enhancing CubeSat communication, power, and payload capabilities. As CubeSats continue to advance, it is expected that more comprehensive case studies of integrated antenna systems will emerge, further solidifying this approach's viability and utility.

VI. CONCLUSION

This paper has presented a comprehensive review of the design and architecture of CubeSat transceivers. Four design approaches have been identified and reviewed. We compared the performance of the four approaches based on several metrics. Custom SDR systems perform well overall, with lower implementation costs, good reconfigurability, scalability, and moderate size and complexity. Commercial SDR systems have slightly higher data rates, better power efficiency, and shorter development time, but at higher costs. Commercial hardware systems achieve the highest data rates, reaching up to nearly 1.7 Gbps, but have the highest power consumption, up to 50 W, larger sizes, and limited reconfigurability. Custom hardware systems vary in performance, with some exhibiting lower data rates and higher power consumption. The comparison should be interpreted within the context of the reviewed CubeSat systems. Most reviewed systems employed QPSK modulation and used forward error correction schemes. However, only two systems used encryption for the command uplink signals. The S-band and VHF/UHF bands were the most commonly used bands among the reviewed systems, and generally among all launched CubeSats, while the X-band was the least common among the reviewed systems. However, there is a trend towards moving to higher frequency bands as reflected from the number of reviewed systems that operate over the Ka-band.

CubeSat transceivers still face many challenges, namely the development of energy-efficient high-speed modems

that satisfy CubeSats' constraints. The need for high-speed connectivity is becoming increasingly more essential with the rapid increase in the number of commercial CubeSat launches. Several directions for moving forward have been identified and discussed such as the use of improved coding algorithms, use of FPGAs, employment of multiple access techniques, employment of beamforming and MIMO, use of advanced antennas, and transition to higher frequency bands. With such improvements and technology developments, the future of CubeSats seems very promising in playing a major role in global wireless communications with applications ranging from high-speed connectivity, smart cities, IoT services, and many other uprising civil and commercial applications.

ACKNOWLEDGMENT

Open Access Funding provided by the Qatar National Library, QNL. The contents herein are solely the responsibility of the authors.

REFERENCES

[1] F. E. Tubbal, R. Raad, and K.-W. Chin, "A survey and study of planar antennas for pico-satellites," *IEEE Access*, vol. 3, pp. 2590–2612, 2015.

[2] K. Ramahatla, M. Mosalaosi, A. Yahya, and B. Basutli, "Multiband reconfigurable antennas for 5G wireless and CubeSat applications: A review," *IEEE Access*, vol. 10, pp. 40910–40931, 2022.

[3] I. F. Akyildiz, A. Kak, and S. Nie, "6G and beyond: The future of wireless communications systems," *IEEE Access*, vol. 8, pp. 133995–134030, 2020.

[4] M. Centenaro, C. E. Costa, F. Granelli, C. Sacchi, and L. Vangelista, "A survey on technologies, standards and open challenges in satellite IoT," *IEEE Commun. Surveys Tuts.*, vol. 23, no. 3, pp. 1693–1720, 3rd Quart., 2021.

[5] A. Kak and I. F. Akyildiz, "Designing large-scale constellations for the Internet of Space Things with CubeSats," *IEEE Internet Things J.*, vol. 8, no. 3, pp. 1749–1768, Feb. 2021.

[6] A. J. Ali, M. Khalily, A. Sattarzadeh, A. Massoud, M. O. Hasna, T. Khattab, O. Yurduseven, and R. Tafazolli, "Power budgeting of LEO satellites: An electrical power system design for 5G missions," *IEEE Access*, vol. 9, pp. 113258–113269, 2021.

[7] Y. Rahmat-Samii, V. Manohar, and J. M. Kovitz, "For satellites, think small, dream big: A review of recent antenna developments for CubeSats," *IEEE Antennas Propag. Mag.*, vol. 59, no. 2, pp. 22–30, Apr. 2017.

[8] S. Gao, Y. Rahmat-Samii, R. E. Hodges, and X.-X. Yang, "Advanced antennas for small satellites," *Proc. IEEE*, vol. 106, no. 3, pp. 391–403, Mar. 2018.

[9] F. Davoli, C. Kourogiorgas, M. Marchese, A. Panagopoulos, and F. Patrone, "Small satellites and CubeSats: Survey of structures, architectures, and protocols," *Int. J. Satell. Commun. Netw.*, vol. 37, no. 4, pp. 343–359, Jul. 2019.

[10] S. C. Burleigh, T. D. Cola, S. Morosi, S. Jayousi, E. Cianca, and C. Fuchs, "From connectivity to advanced Internet services: A comprehensive review of small satellites communications and networks," *Wireless Commun. Mobile Comput.*, vol. 2019, pp. 1–17, May 2019.

[11] N. Saeed, A. Elzanaty, H. Almorad, H. Dahrouj, T. Y. Al-Naffouri, and M.-S. Alouini, "CubeSat communications: Recent advances and future challenges," *IEEE Commun. Surveys Tuts.*, vol. 22, no. 3, pp. 1839–1862, 3rd Quart., 2020.

[12] O. Kodheli, E. Lagunas, N. Maturo, S. K. Sharma, B. Shankar, J. F. M. Montoya, J. C. M. Duncan, D. Spano, S. Chatzinotas, S. Kisseleff, J. Querol, L. Lei, T. X. Vu, and G. Goussetis, "Satellite communications in the new space era: A survey and future challenges," *IEEE Commun. Surveys Tuts.*, vol. 23, no. 1, pp. 70–109, 1st Quart., 2021.

[13] E. Kulu. (2022). *Nanosats Database*. Accessed: Mar. 25, 2023. [Online]. Available: https://www.nanosats.eu/

[14] A. Edpuganti, V. Khadkikar, M. S. E. Moursi, H. Zeineldin, N. Al-Sayari, and K. Al Hosani, "A comprehensive review on CubeSat electrical power system architectures," *IEEE Trans. Power Electron.*, vol. 37, no. 3, pp. 3161–3177, Mar. 2022.

[15] H. H. Abdullah, A. Elboushi, A. E. Gohar, and E. A. Abdallah, "An improved S-band CubeSat communication subsystem design and implementation," *IEEE Access*, vol. 9, pp. 45123–45136, 2021.

[16] H. Wang, Y. B. Park, and I. Park, "Low-profile wideband solar-cell-integrated circularly polarized CubeSat antenna for the Internet of Space Things," *IEEE Access*, vol. 10, pp. 61451–61462, 2022.

[17] Y.-S. Chen, Y.-H. Wu, and C.-C. Chung, "Solar-powered active integrated antennas backed by a transparent reflectarray for CubeSat applications," *IEEE Access*, vol. 8, pp. 137934–137946, 2020.

[18] M. Yaqoob, A. Lashab, J. C. Vasquez, J. M. Guerrero, M. E. Orchard, and A. D. Bintoudi, "A comprehensive review on small satellite microgrids," *IEEE Trans. Power Electron.*, vol. 37, no. 10, pp. 12741–12762, Oct. 2022.

[19] A. K. El Allam, A. M. Jallad, M. Awad, M. Takruri, and P. R. Marpu, "A highly modular software framework for reducing software development time of nanosatellites," *IEEE Access*, vol. 9, pp. 107791–107803, 2021.

[20] B. Hussein, A. M. Massoud, and T. Khattab, "Centralized, distributed, and module-integrated electric power system schemes in CubeSats: Performance assessment," *IEEE Access*, vol. 10, pp. 55396–55407, 2022.

[21] M. J. Shehab, I. Kassem, A. A. Kutty, M. Kucukvar, N. Onat, and T. Khattab, "5G networks towards smart and sustainable cities: A review of recent developments, applications and future perspectives," *IEEE Access*, vol. 10, pp. 2987–3006, 2022.

[22] S. Abulgasem, F. Tubbal, R. Raad, P. I. Theoharis, S. Lu, and S. Iranmanesh, "Antenna designs for CubeSats: A review," *IEEE Access*, vol. 9, pp. 45289–45324, 2021.

[23] P. Bouça, J. N. Matos, S. R. Cunha, and N. B. Carvalho, "Low-profile aperture-coupled patch antenna array for CubeSat applications," *IEEE Access*, vol. 8, pp. 20473–20479, 2020.

[24] I. Firmansyah and Y. Yamaguchi, "OpenCL implementation of FPGA-based signal generation and measurement," *IEEE Access*, vol. 7, pp. 48849–48859, 2019.

[25] T. Zhang, J. Wang, S. Guo, and Z. Chen, "A comprehensive FPGA reverse engineering tool-chain: From bitstream to RTL code," *IEEE Access*, vol. 7, pp. 38379–38389, 2019.

[26] J. Matondang and Y. Adityawarman, "Implementation of APRS network using LoRa modulation based KISS TNC," in *Proc. Int. Conf. Radar, Antenna, Microw., Electron., Telecommun. (ICRAMET)*, Nov. 2018, pp. 37–40.

[27] K. Varnavas, W. H. Sims, and J. Casas, *The Use of Field Programmable Gate Arrays (FPGA) in Small Satellite Communication Systems*. Washington, DC, USA: NASA Technical Reports Server (NTRS), 2015.

[28] E. Calore and S. F. Schifano, "FER: A benchmark for the roofline analysis of FPGA based HPC accelerators," *IEEE Access*, vol. 10, pp. 94220–94234, 2022.

[29] V. K. Garg, "Fourth generation systems and new wireless technologies," *Wireless Commun. Netw.*, vol. 23, no. 1, pp. 1–22, Oct. 2007.

[30] J. T. Gómez, Y. J. Naranjo, F. Dressler, and M. J. F.-G. García, "Undergraduate curriculum to teach and provide research skills on hardware design for SDR applications in FPGA technology," *IEEE Access*, vol. 9, pp. 93967–93975, 2021.

[31] L. Tsoeunyane, S. Winberg, and M. Inggs, "Software-defined radio FPGA cores: Building towards a domain-specific language," *Int. J. Reconfigurable Comput.*, vol. 2017, p. 128, Jul. 2017.

[32] P. I. Theoharis, R. Raad, F. Tubbal, M. U. Ali Khan, and S. Liu, "Software-defined radios for CubeSat applications: A brief review and methodology," *IEEE J. Miniaturization Air Space Syst.*, vol. 2, no. 1, pp. 10–16, Mar. 2021.

[33] P. Flak, "Hardware-accelerated real-time spectrum analyzer with a broadband fast sweep feature based on the cost-effective SDR platform," *IEEE Access*, vol. 10, pp. 110934–110946, 2022.

[34] *Digital Video Broadcasting (DVB); Second Generation Framing Structure, Channel Coding and Modulation*, document DVB-S2, Doc. No. ETSI EN 302 307-1 V1.4.1, European Telecommunications Standards Institute (ETSI), Sophia-Antipolis, France, 2014.

[35] K. S. Chan, A. James, and S. Rahardja, "Evaluation of a joint detector demodulator decoder (JDDD) performance with modulation schemes specified in the DVB-S2 standard," *IEEE Access*, vol. 7, pp. 86217–86225, 2019.

[36] M. Tropea, F. De Rango, and A. F. Santamaria, "Design of a two-stage scheduling scheme for DVB-S2/S2X satellite architecture," *IEEE Trans. Broadcast.*, vol. 67, no. 2, pp. 424–437, Jun. 2021.

[37] K. Devaraj, R. Kingsbury, M. Ligon, J. Breu, V. Vittaldev, B. Klofas, P. Yeon, and K. Colton, "Dove high speed downlink system," in *Proc. 31st Annu. AIAA/USU Conf. Small Satell.*, 2017, pp. 1–9.

[38] J. DeSanto and D. Hei, "CubeSat communication architectures: Recent trends and future directions," in *Proc. IEEE Aerosp. Conf.*, Sep. 2015, pp. 1–12.

[39] D. Roth, "Development of a CCSDS space packet protocol (SCSP) software stack for CubeSats," in *Proc. IEEE Int. Conf. Space Mission Challenges for Inf. Technol. (SMC-IT)*, Sep. 2016, pp. 26–34.

[40] P. Kuzmenko, "Integration of the CCSDS space packet protocol into spacecraft onboard software," in *Proc. Int. Conf. Adv. Comput. Inf. Technol. (ACIT)*, 2017, pp. 107–111.

[41] E. Ledergerber, "CubeSat satellite communication architecture: CCSDS and DTN protocols," in *Proc. IEEE Aerosp. Conf.*, Sep. 2018, pp. 1–9.

[42] S. Gao, "Design and implementation of CubeSat communication system based on CCSDS protocol stack," in *Proc. Int. Conf. Space Commun., Navigat. Earth Observ. Syst. (ICSCN)*, Jul. 2020, pp. 1–5.

[43] J. Fang, X. Bu, and K. Yang, "Retransmission spurts of deferred NAK ARQ in fountain coding aided CCSDS file-delivery protocol," *IEEE Commun. Lett.*, vol. 20, no. 4, pp. 816–819, Apr. 2016.

[44] J. Liu and Q. Feng, "A miniaturized LDPC encoder: Two-layer architecture for CCSDS near-earth standard," *IEEE Trans. Circuits Syst. II, Exp. Briefs*, vol. 68, no. 7, pp. 2384–2388, Jul. 2021.

[45] P. Chatziantoniou, A. Tsigkanos, D. Theodoropoulos, N. Kranitis, and A. Paschalis, "An efficient architecture and high-throughput implementation of CCSDS-123.0-B-2 hybrid entropy coder targeting space-grade SRAM FPGA technology," *IEEE Trans. Aerosp. Electron. Syst.*, vol. 58, no. 6, pp. 5470–5482, Dec. 2022.

[46] M. Yongkui, Z. Zhongzhao, and Z. Naitong, "Simulation for CCSDS advanced orbiting system (AOS) with BONeS designer," *J. Syst. Eng. Electron.*, vol. 14, no. 1, pp. 92–96, Mar. 2003.

[47] S. M. Dilek, A. Ayranci, A. Seker, O. Ceylan, and H. B. Yagci, "AX.25 protocol compatible reconfigurable 2/4 FSK modulator design for nano/micro-satellites," in *Proc. 20th Telecommun. Forum (TELFOR)*, Nov. 2012, pp. 416–419.

[48] J. J. Paternina-Anaya, J. E. Salamanca-Céspedes, and M. A. Ávila-Angulo, "Communication system design and implementation for one pico-satellite and four Earth stations using AX.25," in *Proc. IEEE Central Amer. Panama Conv. (CONCAPAN XXXIV)*, Nov. 2014, pp. 1–6.

[49] A. Skrastins, J. Jelinski, and G. Lauks, "Evaluation of new approach for fair downlink bandwidth distribution in TCP/IP networks," in *Proc. IET Int. Conf. Inf. Commun. Technol. (IETICT)*, Apr. 2013, pp. 117–123.

[50] L. Charaabi and I. Jaziri, "Designing a tiny and customizable TCP/IP core for low cost FPGA," in *Proc. Int. Conf. Eng. MIS (ICEMIS)*, May 2017, pp. 1–6.

[51] F. Xiao and Z. Zhu, "Research of embedded WebServer based on CAN-TCP/IP gateway," in *Proc. Int. Conf. Intell. Sci. Inf. Eng.*, Aug. 2011, pp. 279–281.

[52] V. A. Delgado-Gallardo, R. Sandoval-Arechiga, and R. Parra-Michel, "A top-down modeling approach for networks-on-chip components design: A switch as case study," *IEEE Access*, vol. 11, pp. 4412–4433, 2023.

[53] P. Flak, "Drone detection sensor with continuous 2.4 GHz ISM band coverage based on cost-effective SDR platform," *IEEE Access*, vol. 9, pp. 114574–114586, 2021.

[54] M. R. Maheshwarappa, M. Bowyer, and C. P. Bridges, "Software defined radio (SDR) architecture to support multi-satellite communications," in *Proc. IEEE Aerosp. Conf.*, Mar. 2015, pp. 1–10.

[55] M. R. Maheshwarappa and C. P. Bridges, "Software defined radios for small satellites," in *Proc. NASA/ESA Conf. Adapt. Hardw. Syst. (AHS)*, Jul. 2014, pp. 172–179.

[56] C. Bridges, S. Kenyon, C. Underwood, and V. Lappas, "STRaND-1: The world's first smartphone nanosatellite," in *Proc. 2nd Int. Conf. Space Technol.*, Sep. 2011, pp. 1–3.

[57] M. R. Maheshwarappa, M. D. J. Bowyer, and C. P. Bridges, "Improvements in CPU & FPGA performance for small satellite SDR applications," *IEEE Trans. Aerosp. Electron. Syst.*, vol. 53, no. 1, pp. 310–322, Feb. 2017.

[58] M. R. Maheshwarappa, M. D. J. Bowyer, and C. P. Bridges, "A reconfigurable SDR architecture for parallel satellite reception," *IEEE Aerosp. Electron. Syst. Mag.*, vol. 33, no. 11, pp. 40–53, Nov. 2018.

[59] X. Cai, M. Zhou, T. Xia, W. H. Fong, W.-T. Lee, and X. Huang, "Low-power SDR design on an FPGA for intersatellite communications," *IEEE Trans. Very Large Scale Integr. (VLSI) Syst.*, vol. 26, no. 11, pp. 2419–2430, Nov. 2018.

[60] J. Downey and T. Kacpura, "Pre-flight testing and performance of a Ka-band software defined radio," in *Proc. 30th AIAA Int. Commun. Satell. Syst. Conf. (ICSSC)*, Sep. 2012, p. 113.

[61] G. Wu, Y. Bai, and Z. Sun, "Research on formation of microsatellite communication with genetic algorithm," *Sci. World J.*, vol. 2013, no. 4, p. 17, Sep. 2013.

[62] W. Edmonson, S. Gebreyohannes, A. Dillion, R. Radhakrishnan, J. Chenou, A. Esterline, and F. Afghah, "Systems engineering of inter-satellite communications for distributed systems of small satellites," in *Proc. Annu. IEEE Syst. Conf. (SysCon)*, Apr. 2015, pp. 705–710.

[63] B. Butters and R. Raad, "A 2.4 GHz high data rate radio for pico-satellites," in *Proc. 8th Int. Conf. Telecommun. Syst. Services Appl. (TSSA)*, Oct. 2014, pp. 1–6.

[64] O. Popescu, "Power budgets for CubeSat radios to support ground communications and inter-satellite links," *IEEE Access*, vol. 5, pp. 12618–12625, 2017.

[65] E. Grayver, A. Chin, J. Hsu, S. Stanev, D. Kun, and A. Parower, "Software defined radio for small satellites," in *Proc. IEEE Aerosp. Conf.*, Mar. 2015, pp. 1–9.

[66] J. H. Lee, S. H. Liu, C. J. Mann, J. C. Nocerino, D. Walker, J. B. Blake, W. R. Crain, A. L. Berman, G. Kinum, V. L. Chin, M. D. Looper, M. Mellick, J. A. Tardif, C. M. Coffman, B. S. Hardy, and D. A. Hinkley, "First on-orbit results from the AeroCube-10 space solar cell experiment," in *Proc. 47th IEEE Photovoltaic Spec. Conf. (PVSC)*, Jun. 2020, pp. 1738–1741.

[67] J. H. Lee, C. J. Mann, D. Walker, D. L. Turner, J. B. Blake, W. R. Crain, D. A. Hinkley, M. Mellick, B. S. Hardy, and S. H. Liu, "Ground testing and instrument development for the AeroCube-10 space solar cell experiment," in *Proc. IEEE 7th World Conf. Photovoltaic Energy Convers. (WCPEC) (A Joint Conf. 45th IEEE PVSC, 28th PVSEC 34th EU PVSEC)*, Jun. 2018, pp. 3364–3366.

[68] A. Haghighat, "A review on essentials and technical challenges of software defined radio," in *Proc. MILCOM*, Oct. 2002, pp. 377–382.

[69] E. Schmidt, Z. Ruble, D. Akopian, and D. J. Pack, "Software-defined radio GNSS instrumentation for spoofing mitigation: A review and a case study," *IEEE Trans. Instrum. Meas.*, vol. 68, no. 8, pp. 2768–2784, Aug. 2019.

[70] R. Akeela and B. Dezfouli, "Software-defined radios: Architecture, state-of-the-art, and challenges," *Comput. Commun.*, vol. 128, pp. 106–125, Sep. 2018.

[71] N. Hosseini and D. W. Matolak, "Software defined radios as cognitive relays for satellite ground stations incurring terrestrial interference," in *Proc. Cognit. Commun. Aerosp. Appl. Workshop (CCAA)*, Jun. 2017, pp. 1–4.

[72] R. Olive, A. Amezaga, H. Carreno-Luengo, H. Park, and A. Camps, "Implementation of a GNSS-R payload based on software-defined radio for the 3CAT-2 mission," *IEEE J. Sel. Topics Appl. Earth Observ. Remote Sens.*, vol. 9, no. 10, pp. 4824–4833, Oct. 2016.

[73] H. Carreno-Luengo, A. Camps, P. Via, J. F. Munoz, A. Cortiella, D. Vidal, J. Jane, N. Catarino, M. Hagenfeldt, P. Palomo, and S. Cornara, "3CAT-2—An experimental nanosatellite for GNSS-R Earth observation: Mission concept and analysis," *IEEE J. Sel. Topics Appl. Earth Observ. Remote Sens.*, vol. 9, no. 10, pp. 4540–4551, Oct. 2016.

[74] H. Carreno-Luengo, A. Amèzaga, A. Bolet, D. Vidal, J. Jané, J. F. Munoz, R. Olivé, A. Camps, J. Carola, N. Catarino, M. Hagenfeldt, P. Palomo, and S. Cornara, "3CAT-2: A 6U CubeSat-based multi-constellation, dual-polarization, and dual-frequency GNSS-R and GNSS-RO experimental mission," in *Proc. IEEE Int. Geosci. Remote Sens. Symp. (IGARSS)*, Jul. 2015, pp. 5115–5118.

[75] J. Castellví, A. Camps, J. Corbera, and R. Alamús, "3Cat-3/MOTS nanosatellite mission for optical multispectral and GNSS-R Earth observation: Concept and analysis," *Sensors*, vol. 18, no. 2, p. 140, Jan. 2018.
[76] J. F. Munoz-Martin, N. Miguelez, R. Castella, L. Fernandez, A. Solanellas, P. Via, and A. Camps, "3Cat-4: Combined GNSS-R, L-band radiometer with RFI mitigation, and AIS receiver for a I-unit CubeSat based on software defined radio," in *Proc. IEEE Int. Geosci. Remote Sens. Symp.*, Jul. 2018, pp. 1063–1066.
[77] J. A. Ruiz-de-Azua, J. F. Muñoz, L. Fernández, M. Badia, D. Llavería, C. Diez, A. Aguilella, A. Pérez, O. Milian, M. Sobrino, A. Navarro, H. Lleó, M. Sureda, M. Soria, A. Calveras, and A. Camps, "3Cat-4 mission: A 1-Unit CubeSat for Earth observation with a L-band radiometer and a GNSS-reflectometer using software defined radio," in *Proc. IEEE Int. Geosci. Remote Sens. Symp.*, Jul. 2019, pp. 8867–8870.
[78] K. Aigul, A. Altay, D. Yevgeniya, M. Bekbolat, and O. Zhadyra, "Improvement of signal reception reliability at satellite spectrum monitoring system," *IEEE Access*, vol. 10, pp. 101399–101407, 2022.
[79] F. Alimenti et al., "K/Ka-band very high data-rate receivers: A viable solution for future moon exploration missions," *Electronics*, vol. 8, no. 3, p. 349, Mar. 2019.
[80] E. Kneller, K. Hyer, T. McIntyre, D. Jones, and C. Swenson, "Cadet: A high data rate software defined radio for smallsat applications," in *Proc. 26th Annu. AIAA/USU Conf. Small Satell.*, 2012, pp. 1–10.
[81] C. Fish, "DICE mission design, development, and implementation: Success and challenges," in *Proc. 26th Annu. AIAA/USU Conf. Small Satell.*, 2012, pp. 11–30.
[82] Z. Katona, M. Gräßlin, A. Donner, N. Kranich, H. Brandt, H. Bischl, and M. Brück, "A flexible LEO satellite modem with Ka-band RF frontend for a data relay satellite system," *Int. J. Satell. Commun. Netw.*, vol. 38, no. 3, pp. 301–313, May 2020.
[83] M. Kishimoto, T. Malmadayalage, A. Maskey, P. Lepcha, D. Withanage, Y. Kakimoto, Y. Sasaki, H. Shrestha, G. Maeda, T. Yamauchi, S. Kim, H. Masui, and M. Cho, "Improvement of communication system for 1U CubeSat," in *Proc. 34th Annu. Small Satell. Conf.*, 2020, pp. 1–8.
[84] Md. Samsuzzaman, M. T. Islam, S. Kibria, and M. Cho, "BIRDS-1 CubeSat constellation using compact UHF patch antenna," *IEEE Access*, vol. 6, pp. 54282–54294, 2018.
[85] Y. Yin, K. El-Sankary, Z. Chen, Y. Gao, M. I. Vai, and S.-H. Pun, "An intermittent frequency synthesizer with accurate frequency detection for fast duty-cycled receivers," *IEEE Access*, vol. 8, pp. 45148–45155, 2020.
[86] Y. Liu, D. Ren, F. Yan, Z. Wu, Z. Dong, and Y. Chen, "Performance comparison of power divider and fiber splitter in the fiber-based frequency transmission system of solar radio observation," *IEEE Access*, vol. 9, pp. 24925–24932, 2021.
[87] K. Pradhan, F. Pauline, G. Maeda, S. Kim, H. Masui, and M. Cho, "BIRDS-2: Multi-Nation CubeSat constellation project for learning and capacity building," in *Proc. 32nd Annu. AIAA/USU Conf. Small Satell.*, 2018, pp. 1–9.
[88] M. H. Azami, G. Maeda, P. Faure, T. Yamauchi, S. Kim, H. Masui, and M. Cho, "BIRDS-2: A constellation of joint global multi-nation 1U CubeSats," *J. Phys., Conf. Ser.*, vol. 1152, Jan. 2019, Art. no. 012008.
[89] S. B. M. Zaki, M. H. Azami, T. Yamauchi, S. Kim, H. Masui, and M. Cho, "Design, analysis and testing of monopole antenna deployment mechanism for BIRDS-2 CubeSat applications," *J. Phys., Conf. Ser.*, vol. 1152, Jan. 2019, Art. no. 012007.
[90] S. E. Palo, "High rate communications systems for CubeSats," in *IEEE MTT-S Int. Microw. Symp. Dig.*, May 2015, pp. 1–4.
[91] S. Rogers, J. Vega, Y. Zenkov, C. Knoblauch, D. Bautista, T. Bautista, R. Fagan, C. Roberson, S. Flores, R. Barakat, V. Chacko, J. Gamaunt, A. Acuna, J. D. Bowman, and D. C. Jacobs, "Phoenix: A CubeSat mission to study the impact of urban heat islands within the U.S.," in *Proc. 34th Annu. Small Satell. Conf.*, 2020, pp. 9–17.
[92] C. Spells, S. Doucette, and A. Ketsdever, "Bio-inspired engineering for the exploration of remote worlds," in *Proc. IEEE Aerosp. Conf.*, Mar. 2015, pp. 1–9.
[93] E. Stoll, H. Konstanski, C. Anderson, K. Douglass, and M. Oxfort, "The RapidEye constellation and its data products," in *Proc. IEEE Aerosp. Conf.*, Mar. 2012, pp. 1–9.
[94] E. Zillmann and H. Weichelt, "Grassland identification using multi-temporal RapidEye image series," in *Proc. MultiTemp, 7th Int. Workshop Anal. Multi-Temporal Remote Sens. Images*, Jun. 2013, pp. 1–4.
[95] A. Marx and G. O. Tetteh, "A forest vitality and change monitoring tool based on RapidEye imagery," *IEEE Geosci. Remote Sens. Lett.*, vol. 14, no. 6, pp. 801–805, Jun. 2017.
[96] C. R. Boshuizen, J. Mason, P. Klupar, and S. Spanhake, "Results from the planet labs flock constellation," in *Proc. 28th Annu. AIAA/USU Conf. Small Satell.*, 2014, pp. 1–8.
[97] D. Doan, R. Zimmerman, L. Leung, J. Mason, N. Parsons, and K. Shahid, "Commissioning the world's largest satellite constellation," in *Proc. 31st Annu. AIAA/USU Conf. Small Satell.*, 2017, pp. 1–10.
[98] K. Devaraj. (2049). *B14: The CubeSat With One of the World's Fastest Satellite Radios*. Planet. Accessed: Mar. 28, 2023. [Online]. Available: https://www.planet.com
[99] K. Devaraj, M. Ligon, E. Blossom, J. Breu, B. Klofas, K. Colton, and R. Kingsbury, "Planet high speed radio: Crossing Gbps from a 3U CubeSat," in *Proc. 33rd Annu. AIAA/USU Conf. Small Satell.*, 2019, pp. 1–10.
[100] K. Leveque, L. Carleton, J. King, Z. Cuseo, and R. Babb, "Unlocking the next generation of nano-satellite missions with 320 Mbps Ka-band downlink: On-orbit results," in *Proc. 33rd Annu. AIAA/USU Conf. Small Satell.*, 2019, pp. 30–40.
[101] R. Hodges, D. Lewis, M. Radway, A. Toorian, F. Aguirre, D. Hoppe, B. Shah, A. Gray, D. Rowen, R. Welle, A. Kalman, A. Reif, and J. Martin, "The ISARA mission flight demonstration of a high gain Ka-band antenna for 100 Mbps telecom," in *Proc. 32nd Annu. AIAA/USU Conf. Small Satell.*, 2018, pp. 76–87.
[102] T. S. Rose, D. W. Rowen, S. Lalumondiere, N. I. Werner, R. Linares, A. Faler, J. Wicker, C. M. Coffman, G. A. Maul, D. H. Chien, A. Utter, R. P. Welle, and S. W. Janson, "Optical communications downlink from a 1.5U CubeSat: OCSD program," in *Proc. Int. Conf. Space Opt. (ICSO)*, Jul. 2019, pp. 201–212.
[103] G. Hunyadi, D. M. Klumpar, S. Jepsen, B. Larsen, and M. Obland, "A commercial off the shelf (COTS) packet communications subsystem for the Montana Earth-orbiting pico-explorer (MEROPE) CubeSat," in *Proc. IEEE Proc. Aerosp. Conf.*, Mar. 2002, p. 1.
[104] J. Schaffner, "The electronic system design, analysis, integration, and construction of the Cal Poly State University CP1 CubeSat," in *Proc. 16th Annu. AIAA/USU Conf. Small Satell.*, 2002, pp. 1–12.
[105] E. B. Zantou and A. Kherras, "Small mobile ground terminal design for a microsatellite data collection system," *J. Aerosp. Comput., Inf., Commun.*, vol. 1, no. 9, pp. 364–371, Sep. 2004.
[106] C. Clark, A. Chin, P. Karuza, D. Rumsey, and D. Hinkley, "CubeSat communications transceiver for increased data throughput," in *Proc. IEEE Aerosp. Conf.*, Mar. 2009, pp. 1–5.
[107] R. Leitch and I. Hemphill, "Sapphire: A small satellite system for the surveillance of space," in *Proc. 24th Annu. AIAA/USU Conf. Small Satell.*, 2010.
[108] A. Addaim, A. Kherras, and E. Bachir, "Design of low-cost telecommunications CubeSat-class spacecraft," *Aerosp. Technol. Advancements*, vol. 1, no. 15, pp. 293-318, Jan. 2010.
[109] P. Muri and J. McNair, "A survey of communication sub-systems for intersatellite linked systems and CubeSat missions," *J. Commun.*, vol. 7, no. 4, pp. 290–308, Apr. 2012.
[110] B. Klofas. (2018). *CubeSat Communications System Table Version 17/Latest*. CubeSat Communications System Table. Accessed Mar. 28, 2023. [Online]. Available: https://www.klofas.com/comm-table/table.pdf
[111] A. Gaysin, V. Fadeev, and M. Hennhofer, "Survey of modulation and coding schemes for application in CubeSat systems," in *Proc. Syst. Signal Synchronization, Generating Process. Telecommun.*, 2017, pp. 1–7.
[112] F. Tubbal, R. Raad, K.-W. Chin, L. Matekovits, B. Butters, and G. Dassano, "A high gain S-band slot antenna with MSS for CubeSat," *Ann. Telecommun.*, vol. 74, nos. 3–4, pp. 223–237, Apr. 2019.
[113] M. J. Zakavi, S. A. Nezamalhosseini, and L. R. Chen, "Multiuser massive MIMO-OFDM for visible light communication systems," *IEEE Access*, vol. 11, pp. 2259–2273, 2023.
[114] R. Radhakrishnan, "Optimal multiple access protocol for intersatellite communication in small satellite systems," *Proc. 4S Symp.*, 2014, pp. 1–15.
[115] F. Pinto, F. Afghah, R. Radhakrishnan, and W. Edmonson, "Software defined radio implementation of DS-CDMA in inter-satellite communications for small satellites," in *Proc. IEEE Int. Conf. Wireless Space Extreme Environ. (WiSEE)*, Dec. 2015, pp. 1–6.

[116] R. Radhakrishnan, W. W. Edmonson, F. Afghah, R. M. Rodriguez-Osorio, F. Pinto, and S. C. Burleigh, "Survey of inter-satellite communication for small satellite systems: Physical layer to network layer view," *IEEE Commun. Surveys Tuts.*, vol. 18, no. 4, pp. 2442–2473, 4th Quart., 2016.
[117] S. S. Arnold, R. Nuzzaci, and A. Gordon-Ross, "Energy budgeting for CubeSats with an integrated FPGA," in *Proc. IEEE Aerosp. Conf.*, Mar. 2012, pp. 1–14.
[118] F. Santoni, F. Piergentili, S. Donati, M. Perelli, A. Negri, and M. Marino, "An innovative deployable solar panel system for CubeSats," *Acta Astronautica*, vol. 95, pp. 210–217, Feb. 2014.
[119] F. Santoni, F. Piergentili, S. Donati, M. Perelli, A. Negri, and M. Marino, "Design and realization of an innovative deployable solar panel system for CubeSats," in *Proc. 63rd Int. Astron. Congr.*, Naples, Italy, Oct. 2012, pp. 7119–7127.
[120] J. Plaza, J. Vilan, F. Agelet, J. Mancheno, M. Estevez, C. Fernandez, and F. Ares, "Xatcobeo: Small mechanisms for CubeSat satellites antenna and solar array deployment," in *Proc. 40th Aerosp. Mech. Symp.*, May 2010, pp. 415–429.
[121] M. Passaretti and R. Hayes, "Development of a solar array drive assembly for CubeSat," in *Proc. 40th Aerosp. Mech. Symp.*, May 2010, pp. 445–453.
[122] A. Reif, V. Hoang, and A. Kalman, "Recent advances in the construction of solar arrays for CubeSats," in *Proc. 24th Annu. AIAA/USU Conf. Small Satell.*, 2010, pp. 53–71.
[123] K. Alrushud, V. G. Buendìa, and S. K. Podilchak, "Planar quasi-end-fire antenna design using SIW technology for CubeSats and other small satellites," in *Proc. 15th Eur. Conf. Antennas Propag. (EuCAP)*, Mar. 2021, pp. 1–5.
[124] X. Li, L. Wang, J. Wang, and G. Goussetis, "Conformal high gain aperture antenna based on leaky-wave array for CubeSat communication," in *Proc. Int. Symp. Antennas Propag. (ISAP)*, Jan. 2021, pp. 499–500.
[125] D. Kim, M. Hwang, G. Kim, and S. Kim, "Self-deployable circularly polarized phased Yagi–Uda antenna array using 3-D printing technology for CubeSat applications," *IEEE Antennas Wireless Propag. Lett.*, vol. 21, no. 11, pp. 2249–2253, Nov. 2022.
[126] N. Meirambekuly, B. A. Karibayev, T. A. Namazbayev, G. A. E. Ibrayev, S. O. Orynbassar, S. A. Ivanovich, and A. A. Temirbayev, "A high gain deployable L/S band conical helix antenna integrated with optical system for Earth observation CubeSats," *IEEE Access*, vol. 11, pp. 23097–23106, 2023.
[127] W. Alomar, J. Degnan, S. Mancewicz, M. Sidley, J. Cutler, and B. Gilchrist, "An extendable solar array integrated Yagi–Uda UHF antenna for CubeSat platforms," in *Proc. IEEE Int. Symp. Antennas Propag. (APSURSI)*, Jul. 2011, pp. 3022–3024.
[128] C. Chen, "A dual-band circularly polarized shared-aperture antenna for 1U CubeSat applications," *IEEE Trans. Antennas Propag.*, vol. 70, no. 5, pp. 3818–3823, May 2022.
[129] T. R. Jones, J. P. Grey, and M. Daneshmand, "Solar panel integrated circular polarized aperture-coupled patch antenna for CubeSat applications," *IEEE Antennas Wireless Propag. Lett.*, vol. 17, no. 10, pp. 1895–1899, Oct. 2018.

AMR ZEEDAN received the B.S. degree in electrical engineering from Qatar University, Doha, Qatar, in 2021, where he is currently pursuing the M.Sc. degree in electrical engineering. From 2020 to 2021, he was an Undergraduate Research Assistant with the Department of Electrical Engineering, Qatar University, where he has been a Graduate Research Assistant, since August 2021. His research interests include the IoT-based smart systems, signal processing, sustainable solar energy development, digital communication system design, small satellite communications, and quantum communication. He has been awarded the Amiri Undergraduate Academic Excellence Scholarship during the undergraduate study and the Graduate Sponsorship Research Award (GSRA) from the Qatar National Research Fund (QNRF) covering the two-year period of the current graduate program.

TAMER KHATTAB (Senior Member, IEEE) received the B.Sc. and M.Sc. degrees in electronics and communications engineering from Cairo University, Giza, Egypt, and the Ph.D. degree in electrical and computer engineering from The University of British Columbia (UBC), Vancouver, BC, Canada, in 2007. From 1994 to 1999, he was with IBM WTC, Giza, as a Development Team Member, and then as the Development Team Lead. From 2000 to 2003, he was with Nokia (formerly Alcatel Canada Inc.), Burnaby, BC, Canada, as a Senior Member of the Technical Staff. From 2006 to 2007, he was a Postdoctoral Fellow with The University of British Columbia, where he was involved in prototyping advanced Gbits/s wireless LAN baseband transceivers. In 2007, he joined Qatar University (QU), where he is currently a Professor of electrical engineering. In addition to more than 150 high-profile academic journal and conference publications, he has several published and pending patents. His research interests include physical layer security techniques, information-theoretic aspects of communication systems, radar and RF sensing techniques, and optical communication. He is a Senior Member of the Technical Staff with the Qatar Mobility Innovation Center (QMIC), a research and development center owned by QU and funded by the Qatar Science and Technology Park (QSTP).